DISSERTATIONES
GEOPHYSICALES
UNIVERSITATIS
TARTUENSIS
31

TANEL VOORMANSIK

Long-term datasets of dual-polarisation weather radar help detect and nowcast convective storms including extreme precipitation, lightning, and hail

DISSERTATIONES GEOPHYSICALES UNIVERSITATIS TARTUENSIS
31

DISSERTATIONES GEOPHYSICALES UNIVERSITATIS TARTUENSIS
31

TANEL VOORMANSIK

Long-term datasets of dual-polarisation weather radar help detect and nowcast convective storms including extreme precipitation, lightning, and hail

UNIVERSITY OF TARTU
Press
1632

Institute of Physics, Faculty of Science and Technology, University of Tartu, Estonia

Dissertation was accepted for the commencement of the degree of *Doctor philosophiae* in environmental technology at the University of Tartu on 12.06.2023 to 15.06.2023 by the Scientific Council on Environmental Technology, University of Tartu.

Supervisors:	Piia Post, PhD, Assoc. Prof., Atmospheric Physics Laboratory, Institute of Physics, University of Tartu, Estonia
	Dmitri Moisseev, PhD, Prof., Institute for Atmospheric and Earth System Research, University of Helsinki, Finland
Opponent:	Hidde Leijnse, PhD, Radar Scientist, The Royal Netherlands Meteorological Institute (KNMI), Netherlands
Commencement:	Room B103, W. Ostwaldi Street 1 (Physicum), Tartu, on 25th of August 2023 at 2.15 p.m.

Publication of this thesis is granted by the Institute of Physics, University of Tartu

ISSN 1406-0310 (print)
ISBN 978-9916-27-271-8 (print)
ISSN 2806-2329 (pdf)
ISBN 978-9916-27-272-5 (pdf)

University of Tartu Press
www.tyk.ee

TABLE OF CONTENTS

LIST OF ORIGINAL PUBLICATIONS

This thesis is based on the following publications, which are referred to in the text by their Roman numerals. The full texts are included at the end of the thesis.

I **Voormansik, T.**, Rossi, P.J., Moisseev, D., Tanilsoo, T., Post, P., 2017. Thunderstorm hail and lightning detection parameters based on dual-polarisation Doppler weather radar data. Meteorological Applications 24(3), 521–530.

II **Voormansik, T.**, Cremonini, R., Post, P., Moisseev, D., 2021. Evaluation of the dual-polarisation weather radar quantitative precipitation estimation using long-term datasets. Hydrology and Earth System Sciences 25(3), 1245–1258.

III **Voormansik, T.**, Müürsepp, T., Post, P., 2021. Climatology of convective storms in Estonia from radar data and severe convective environments. Remote Sensing 13(11), 2178.

IV Cremonini, R., **Voormansik, T.**, Post, P., Moisseev, D., 2023. Estimation of extreme precipitation events in Estonia and Italy using dual-polarization weather radar quantitative precipitation estimations. Atmospheric Measurement Techniques 16(11), 2943–2956.

AUTHOR'S CONTRIBUTION TO THE PUBLICATIONS

I **Voormansik, T.**, Rossi, P.J., Moisseev, D., Tanilsoo, T., Post, P., 2017. Thunderstorm hail and lightning detection parameters based on dual-polarisation Doppler weather radar data. Meteorological Applications 24(3), 521–530.

Paper I proposes the best estimators for lightning and hail onset in convective storms from dual-polarisation Doppler weather radar based on 4 years of summer period data in Estonia. The author of the thesis was responsible for the concept of the study and overall scientific work and writing process of the paper.

II **Voormansik, T.**, Cremonini, R., Post, P., Moisseev, D., 2021. Evaluation of the dual-polarisation weather radar quantitative precipitation estimation using long-term datasets. Hydrology and Earth System Sciences 25(3), 1245–1258.

Paper II presents the performance of three weather radar quantitative precipitation estimation methods: a horizontal reflectivity-based product, a specific differential-phase-based product and a combined product based on the previous two. The analysis is based on various accumulation lengths from 1 hour to 1 month from 5 years of summer period data from Italy and Estonia. The author was responsible for the concept and design of the study and carried out the calculations of the Estonian data. He concluded the results and wrote most of the paper.

III **Voormansik, T.**, Müürsepp, T., Post, P., 2021. Climatology of convective storms in Estonia from radar data and severe convective environments. Remote Sensing 13(11), 2178.

Paper III proposes a convective storm definition for the Estonian domain based on weather radar and model data and then constructs a 9-year climatology of convective storms. It also includes synoptic-scale airflow analysis in relation to convective storms. The author of this thesis developed part of the concept and design of the study, carried out radar data processing and analysis and wrote most of the paper.

IV Cremonini, R., **Voormansik, T.**, Post, P., Moisseev, D., 2023. Estimation of extreme precipitation events in Estonia and Italy using dual-polarization weather radar quantitative precipitation estimations. Atmospheric Measurement Techniques 16(11), 2943–2956.

Paper IV introduces intensity-duration-frequency (IDF) curves derived from unadjusted weather radar data. It demonstrated that thanks to the high spatial resolution and accurate high-intensity precipitation estimation by polarimetric radars, even a limited time series of 5 years could provide reliable IDF estimations. The author was responsible for part of the concept and design of the study and carried out the calculations of the Estonian QPE data. He wrote part of the manuscript.

ABSTRACT

Hazardous weather phenomena pose an increasing societal and economic risk throughout the world. Many of those are precipitation-related and can thus be studied using weather radars. The benefits of utilising radars have been proven, especially on phenomena comprising rapid developments and covering small areas which would remain properly unrecorded by traditional observation networks. Such as convective storms involving lightning, hail or flash flood inducing heavy precipitation.

Until the last decade, the vast majority of European operational weather radars were single polarisation radars. While having the spatial and temporal resolution required for severe weather studies, they are limited by various weaknesses inherent to single polarisation radars. Introducing the vertical polarisation in addition to the horizontal in the dual-polarisation weather radars has opened up the potential to improve quantitative precipitation estimation and discriminate between various hydrometeor types more accurately. A number of benefits of the polarimetric radars have not been put into everyday use largely because the operational use of these radars has been relatively short to validate the algorithms properly.

This thesis demonstrates that using an extended dataset of operational dual-polarisation weather radar data enhances our knowledge of various hazardous weather phenomena and thereby helps to increase the quality of the diagnosis and nowcasting even further. It is shown that the accuracy of the quantitative precipitation estimation can be increased by combining specific differential phase and horizontal reflectivity. This radar product improves especially heavy precipitation estimation and thus is also used to derive intensity-duration-frequency curves of short accumulation period of 1-hour.

While convective storms are common phenomena in Estonia in the summer period that cause damage in the region each year, they had never been studied systematically using radar data before. In this work a severe convective storm is defined, and the climatology of those is constructed based on nine years of radar data in conjunction with reanalysis model data and lightning detector data. In addition to heavy rain, convective storms can include lightning and hail. In order to find the best indicator for cloud-to-ground lightning activity, four years of radar data are examined. Proxy hail data from polarimetric hydrometeor classification product are compared to the legacy radar-derived indicator probability of hail to establish a link between the two.

ABBREVIATIONS

List of acronyms

C-band	Frequencies from 4 GHz to 8 GHz
CAPE	Convective available potential energy
CG	Cloud-to-ground flash
ESSL	European Severe Storm Laboratory
ESTEA	Estonian Environment Agency
ESTOFEX	European Storm Forecast Experiment
ET	Echo Top
EUMETNET	European Meteorological Network
GEV	Generalised extreme value
IDF	Intensity-duration-frequency
IPCC	Intergovernmental Panel on Climate Change
JCT	Jenkinson Collison' circulation type
NMS	National Meteorological Service
NORDLIS	Nordic Lightning Information System
POH	Probability of hail
PPI	Plan position indicator
PRF	Pulse repetition frequency
Py-ART	Python ARM Radar Toolkit
QPE	Quantitative precipitation estimation
RHI	Range height indicator
UTC	Coordinated Universal Time
WMO	World Meteorological Organization

List of symbols

ϕ_{DP}	Differential propagation phase
K_{DP}	Specific differential phase
ρ_{HV}	Copolar correlation coefficient
Z_{DR}	Differential reflectivity
Z_{H}	Horizontal reflectivity

1 INTRODUCTION

1.1 Weather radar in hazardous weather phenomena research

Severe weather impacts society and economics in all parts of the globe. According to insurance statistics, nearly 90% of the world's natural disasters are weather-related, and more specifically, the most significant losses are caused by storms, floods, heat waves and wildfires (Vajda et al., 2014). Hazardous weather phenomena are very climate-specific, different parts of the world are exposed to various phenomena. Also, the effect of equal-intensity phenomena can vary depending on the region of its occurrence. There are several ways to classify hazardous weather phenomena. Generally, it depends on risk perception and frequency of occurrence. In the example of the USA, it has been shown that the more frequent tornadoes are in some regions, the lower the casualty counts tend to be (Doswell, 2015). Therefore one can naturally also assume the opposite – the rarer the phenomena for a specific region, the greatest the consequences. The definition of hazardous weather can also vary depending on the field of interest. Even light rain can significantly affect road transport when it falls on ground that is just slightly below freezing point. This illustrates that the severity of weather is an ambiguous concept influenced by the users' requirements, among other factors such as local climate. Arguably hazardous weather phenomena that develop quickly and cannot be forecasted long enough in advance pose the highest risks. Current operational numerical weather models can reliably forecast synoptic-scale hazardous weather phenomena such as heat waves, cold spells or even heavy frontal rainfall several days up to a week ahead. Being prepared for those large-scale phenomena is essential, and forecasting those has significantly benefitted from advances in satellite meteorology, among other factors.

On the other hand, detecting and forecasting small-scale rapidly developing hazardous phenomena have remained challenging. The data and methods available so far have not been able to provide information at the required spatiotemporal scales. In recent decades though, advances in radar meteorology – including especially the introduction of dual-polarisation – have opened up new opportunities. Since the beginning of the usage of weather radars, severe weather like thunderstorms, tornadoes and heavy rainfall events with accompanying floods have prevailed in both the research and operational sides of radar meteorology (Meischner, 2005). This can be considered natural because of the high sampling rate of radars in both space and time, which has given it great benefits over traditional observation networks. In the United States, it has been shown that the introduction of the Weather Surveillance Radar-1988 Doppler (WSR-88D) has significantly improved the short-range forecasts and warnings of severe thunderstorms, tornadoes, and flash floods (Bieringer and Ray, 1996; Polger et al., 1994). Nevertheless, other innovations introduced at about the same time may have also contributed to the improved warning statistics. These include improved numerical

weather models, lightning detectors, new meteorological satellites, wind profiler data and crowdsourced observations (Hintz et al., 2021; Serafin and Wilson, 2000). All of these have been established as key information sources on specific aspects of the atmosphere.

Weather radars are primarily designed for detecting precipitation and associated meteorological phenomena. They function by emitting pulses of electromagnetic energy and detecting the echo returned from scattering objects. The target's location is determined by the delay time the signal travels to and back from the target. The received power estimates a target's reflectivity, mainly known by its link to the precipitation intensity (Meischner, 2005). By using more advanced techniques, it is possible to deduce even more information about the scattering objects. Doppler phase shift enables to determine velocity and direction of movement of the targets. Radar polarimetry allows the particles' size, shape and orientation to be derived (e.g. Bringi and Chandrasekar, 2001; Kumjian, 2013). Severe weather phenomena often develop rapidly and occur in limited spatial dimensions, making weather radar a unique tool in research and operational usage. While weather radar is an excellent source of data, it is also a very demanding and sophisticated instrument. Only well-implemented knowledge-based processing can result in exploiting its true potential. This is a multi-step course including the correct maintenance and calibration of the radar hardware, applying suitable filtering, processing of the data with appropriate methods taking into account local climatology, among other factors, and finally integrating with various other atmospheric data sources depending on the purpose of usage.

1.2 Motivation and aims of the thesis

Many severe weather phenomena are related to precipitation – e.g. convective storms with accompanying lightning, hail and flash floods. There is strengthened evidence since the previous IPCC assessment report AR5 (IPCC, 2014) that the global water cycle will continue to intensify as global temperatures rise and precipitation is projected to become more variable over most land regions within seasons and from year to year. At the global scale, extreme daily precipitation events are projected to intensify by about 7% for each 1 °C global warming until the year 2100 (IPCC, 2021). According to the latest IPCC report (AR6), there is an observed increase in heavy precipitation in Northern Europe, the only region in the world where the confidence in human contribution to the observed change is high (IPCC, 2021). Precipitation amounts are projected to increase even more in the future over high latitudes. Depending on the simulated temperature increase from 1.5 °C to 4 °C, it is going to be up to 20% wetter in Estonia in the next 80 years (IPCC, 2021).

In order to improve the forecasts of any length and type, the source data needs to be reliable. Uncertainties of quantitative precipitation estimations among various datasets (e.g. radar, satellite, rain gauge) can vary highly in different regions, especially in high-intensity events (Fallah et al., 2020; Li et al., 2020; Ukkola

et al., 2020). All of the above clearly indicates the relevance of further increasing our knowledge of the water cycle processes and being better prepared for the consequences of climate change. Increasing the detection and nowcast accuracy of high-intensity events like convective storms, extreme precipitation, hail, and lightning is of the highest importance.

This thesis is devoted to the hazardous summertime weather phenomena in Estonia. Most of these phenomena are related to convective storms, which have not been studied systematically in Estonia before. Therefore a convective storm definition is proposed in **Paper III** using weather radar and atmospheric model data. Based on this, a convective storm climatology is presented. One of the most common threats with convective storms is intense precipitation. **Paper II** presents the comparison of three quantitative precipitation estimation (QPE) methods. A combined approach using both polarimetric and single polarisation data is shown to increase the accuracy based on 5 years of data. In **Paper IV**, intensity-duration-frequency (IDF) curves are derived using the combined QPE approach, and extreme precipitation statistics are provided. In **Paper I**, several radar-based products are studied to determine the best indicators for cloud-to-ground (CG) lightning activity and hail. All four papers benefit from the use of long-term radar datasets. This ensures the robustness of the results, which would be lacking if only selected cases were used. The results of this thesis are aimed to be valuable input for operational use through implementation in the development of nowcasting systems in weather service but also for policymakers and in water management, among other fields.

To summarise, the objectives of this thesis are:

1. Define a severe convective storm for Estonia and provide a convective storm climatology.
2. Improve radar QPE accuracy by using polarimetric data.
3. Advance our understanding of the extreme precipitation climatology in Estonia and compute IDF curves.
4. Define the best radar-based estimators for lightning and hail onset in convective storms.

1.3 Theses

The main scientific contribution of the thesis relates to polarimetric radar data implementation and verification for radar QPE and convective storm analysis using long-term datasets. Specifically, the thesis provides the following new conclusions for the Estonian domain:

- Convective storms were identified with an automated method and analysed regarding synoptic scale conditions. The prevailing airflow direction in the

summer was found to be SW and W, however the highest probability for a severe convective storm is when the airflow is from SE (62%) or S (60%) [III].

- From May to September, the probability of a severe convective storm day for the whole area is 45%, and a thunderstorm day is 54%. In 100 km^2 grid boxes, the probability varies from 1% (2 days per year) in the West Estonian archipelago up to 5% (8 days per year) in continental Estonia [III].
- Above 35 dBZ, nearly 1/3 of the storm areas include lightning, and ¼ include hail [I].
- Convective storm cloud height (echo top with a threshold value of 20 dBZ) is the best estimator for lightning activity [I].
- The QPE product, which combines K_{DP} and Z_H, is proposed, and it is shown that it outperforms either of those separately when compared to rain gauges. In terms of RMSE, it exceeds $R(Z_H)$ by 33% and $R(K_{DP})$ by 69% on average over accumulation lengths from 1 h to 1 month [II].
- The correlation between radar QPE and rain gauges improves with increasing accumulation length from 1 hour to 1 month. The scatter of radar QPE is high in short accumulation lengths due to both systematic and random errors [II].
- High-quality polarimetric radar QPE allows accurate extreme precipitation analysis and estimation of return periods multiple times longer than the underlying data [IV].

2. METHODS

Estonia is located on the eastern coast of the Baltic Sea between 57.5° N and 59.5° N. According to the Köppen climate classification, Estonia belongs to the humid continental climate region, which is generally found between latitudes 30° N and 60° N. In Europe, it covers the central to eastern parts of the continent and southern parts of Scandinavia. The mean annual precipitation amount in Estonia varies from 550 mm in the coastal areas and islands to 750 mm on the windward slopes of the uplands. Precipitation climatology has distinguishable seasonality, the wettest period is summer (mean precipitation over Estonia 215 mm), followed by autumn (198 mm), winter (128 mm), and spring (108 mm), based on the data from 1957–2009 (Tammets and Jaagus, 2013).

In Estonia, hazardous weather phenomena can occur in all seasons, but the most damaging phenomena commonly occur in summer. Most of those are associated with convective storms – heavy (short-term) precipitation, lightning, hail, high winds (downbursts and gust fronts) and relatively rarely also tornadoes (2–3 per year (Kiitsak, 2020)). Other main weather risks actual in the region are blizzards, extreme cold, extreme heat, freezing rain, and drought (Avotniece, 2010; Tammets et al., 2012).

2.1 Detecting convective storms

A convective storm needs several environmental conditions to be met in order to form. It needs high humidity in the boundary layer, nonlocal conditional instability, strong wind shear and a trigger mechanism to cause the lifting of atmospheric boundary-layer air. Numerical weather models can forecast these ingredients sufficiently on a broad scale. Based on these data, forecasters commonly issue warnings over large areas, such as on a country basis, on daily timescales. In Europe, these kinds of warnings provided by National Meteorological Services (NMS) are combined and presented on one website by Meteoalarm (https://meteoalarm.org), which is an initiative by EUMETNET, the European National Meteorological Services Network within the World Meteorological Organization (WMO) (Stepek et al., 2012). Besides that, there are also private initiatives. For example, an unfunded, informal group of meteorologists who developed a severe weather forecasting system in 2002 called the European Storm Forecasting Experiment (ESTOFEX) provides daily forecasts of severe weather with considerable skill based on a scientific forecasting approach (Brooks et al., 2011). In order to contribute to the awareness of convective storms, advance scientific understanding, and foster cooperation within Europe, the European Severe Storms Laboratory (ESSL) initiative has been run since 2006 (Groenemeijer et al., 2017).

Most individual convective storms have a lifespan from a few tens of minutes up to 1 hour and have an area of up to just tens of square kilometres (Kyznarová

and Novák, 2009). This makes it challenging to observe them in real-time or forecast them in advance. Numerical weather models with convective-scale grid spacings of 1–5 km have started to become operational, however the capabilities of those are still limited (Yano et al., 2018). The relatively small size and rapid temporal evolution set specific requirements for the instrumentation needed to study those storms. The temporal and spatial resolution of the measurements has to be high enough to capture different lifecycle phases of the storms, and the measurements should describe various properties of the storm. Ground-based weather stations can provide very accurate temperature, precipitation and wind data, but they are of little use if the storm passes by the station. Thus additional measurement sources are needed to characterise convective storms properly. Nowadays, atmospheric remote sensing instruments have enabled us to make more accurate observations of storms. In addition to providing the required spatiotemporal resolution for these purposes, they can cover large areas, allowing simultaneous data acquisition from multiple convective storms. In this thesis, measurements mostly from weather radar and lightning location systems are applied and studied.

Convective storms are generally detected using the reflectivity data from weather radars, which is related to the part of the storm that includes precipitation (Browning et al., 2007; Goudenhoofdt and Delobbe, 2013; Peter et al., 2015). Moreover, it has been demonstrated that Doppler weather radar provides accurate updraft and downdraft (Figure 1a and 1b) estimations comparable to a wind profiler while fully capturing the storm's three-dimensional structure (Collis et al., 2013). Doppler radar allows showing a localised area of increased convergence immediately preceding rapid storm growth (Wilson and Schreiber, 1986). Characteristic wind profiles have been identified for idealised conceptual models of single-cell, multicell, and supercell convective storms by, e.g. Chisholm and Renick (1972). They found that the structure of those storms was determined mainly by the wind profile of the environment. Weaker and mostly short-lived single-cell storms formed when there was little wind shear. On the other hand, severe (supercell) storm environments were characterised by strong shear. Nevertheless, Doppler wind data from radars is rarely used in operational automatic detection of the convective storms due to low added value compared to the complexity of the integration (e.g. limited useful range due to earth curvature and scan strategy). However, radar wind data has become an integral part of automated tornado detection (Davies-Jones et al., 2020; Durage et al., 2013).

Convective environments favourable for storm development can be retrieved from numerical model data. Convective available potential energy (CAPE) is commonly used as a measure of the degree of instability (Ducrocq et al., 1998). CAPE shows the maximum buoyancy of an undiluted air parcel and is related to the potential updraft strength of thunderstorms. It has to be kept in mind, though, that CAPE can give only an estimate of the strength of a thunderstorm if one forms. It is an essential prerequisite but not a sole or sufficient factor to consider. A triggering process is also needed for a thunderstorm to form. Often even in locations with large CAPE, no thunderstorms form. Still, if thunderstorms are

triggered, larger CAPE denotes higher instability, stronger updrafts and generally more severe thunderstorms (Stull, 2016).

Another challenge is to define what it means for convective storms to be severe. For example, in the United States, a convective storm is considered severe when it produces one or more of the following phenomena at the surface: 1) a tornado, 2) hailstones with a diameter ≥ 2.5 cm, or 3) nontornadic wind gusts ≥ 25 m/s (Brooks et al., 2019). Heavy precipitation is also a criterion in many countries worldwide, but the threshold varies. The thresholds and definitions are often based on a statistical analysis of storm-related measurements and observations. Studies about convective storms have been lacking in Estonia, and the definition of a severe convective storm was missing.

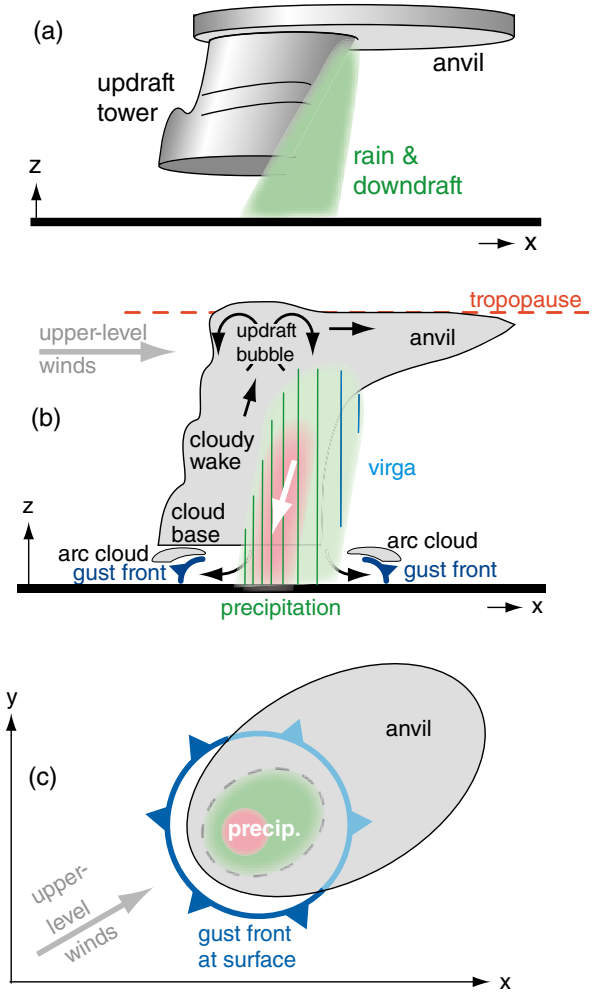

Figure 1. Convective storm in its mature stage. Adapted from Stull (2016).

In order to detect convective storms in an automated and systematic way, also considering the potential operational usage of the method, one has to choose the means to define such storms carefully. Paper III proposes a severe convective storm definition based on radar, lightning detectors, and numerical weather model data. Lightning data is used to verify the thresholds but not in the definition itself. Typically reflectivity thresholds in the range of 30–45 dBZ are applied in reflectivity-based convective storm tracking algorithms (Goudenhoofdt and Delobbe, 2013; Rossi et al., 2014; Seroka et al., 2012). In this thesis 35 dBZ threshold is used for convective cell detection. This is relatively low and thus allows us to monitor convective storms since relatively early phases of the convective system lifecycle. On the other hand, such a low threshold means that also stratiform cells might be included. In order to eliminate non-convective cells, the detected areas were filtered with an increased reflectivity threshold and included CAPE. After testing with various CAPE and reflectivity combinations and comparing the results with CG lightning activity, the following thresholds were chosen for a severe convective storm:

$\geq$ 51 dBZ reflectivity,

$\geq$ 80 J/kg CAPE.

In order to put the reflectivity values into the perspective of rainfall intensity, the convective cell's lower limit, 35 dBZ, translates to about 4.8 mm/h and the threshold for a severe convective storm, 51 dBZ, equals to about 56 mm/h.

2.2 Precipitation measurements in Estonia

The most frequent severe convective storm risk in most parts of the world where convection is a regular phenomenon is heavy rainfall and associated flooding. The basis for all precipitation-related applications and risk management are accurate and homogeneous long-term measurements with high spatiotemporal resolution. In Estonia, precipitation measurements have significantly evolved in the last 70 years. This progress has brought along multiple changes in instrumentation, making obtaining reliable and homogeneous precipitation climatology a complicated task. From 1950 to 2003, traditional manual measurements of precipitation two or four times per day were made using the Tretyakov gauges (Alber et al., 2015). Pluviographs were used in parallel during this period at many stations to record precipitation at a higher temporal resolution of 10 minutes (Tammets and Jakovleva, 2001). The network was updated to automatic tipping-bucket rain gauges from 2003 to 2006. Then starting from 2006, the tipping-bucket gauges were progressively replaced by weighted gauges by the end of 2011. In a comparative study by Alber et al. (2015), it was found that the data from weighted gauges have much higher quality than tipping-bucket gauges. From 2003 to 2011, the data were recorded at 1 h interval. Since 2011 the recording interval has been 10 minutes, but only 1 h data have been quality-controlled by

Estonian Environment Agency (ESTEA) staff. Only 1 h interval gauge data from 2011 and onwards have been used in this thesis to ensure the homogeneity and quality of the measurements. At the time of writing this thesis, there were around 45 OTT Pluvio^2 weighing precipitation gauges (Nemeth, 2008) distributed over the land area of 45 000 km^2 in Estonia. This means, on average, 1 gauge per 1000 km^2. Compared to many other European countries, the network density is low. For example, in Belgium, the network is about 8 times denser as there is 1 gauge per 135 km^2 (Goudenhoofdt and Delobbe, 2009). In Germany, each gauge represents roughly 150 km^2, and in the UK, around 180 km^2 (Lengfeld et al., 2020). Precipitation stations can be classified according to the WMO standards into 5 classes, of which 1 denotes the highest quality (flat horizontal land, surrounded by open area, no uncertainty caused by the surroundings) and 5 the worst (±100% uncertainty) ("Siting Classification | World Meteorological Organization," n.d.). Of the total 45 stations in Estonia, 18 belong to the WMO class 1, 8 belong to class 2, 6 to class 3, 2 to class 4, and the rest are unclassified.

Weather radar measurements have complemented the Estonian precipitation monitoring network since 1975, when the country's first weather radar, MRL-2, was installed in Harku (Kallis et al., 2019). This was replaced by the new Doppler weather radar Gematronic Meteor 500C in 2000. The first currently running modern C-band dual-polarimetric Doppler weather radar, Vaisala WRM200, has been operating in Sürgavere since May 2008 and in Harku since October 2009. Weather radar provides unrivalled spatiotemporal information about precipitation up to several hundred kilometres from the radar site, but it cannot replace traditional gauge measurements due to methodological differences. Radar measures precipitation indirectly and several hundred meters up to several kilometres from the ground level (where gauges are located). It also incorporates several uncertainties originating from various sources, which need to be considered before using the data for QPE. Challenges in the northern European radars include beam blocking, scan strategy, ground and sea clutter, anomalous propagation clutter, gauge adjustment, vertical reflectivity profile (bright band effect), beam overshooting, attenuation by precipitation, overhanging precipitation (Saltikoff et al., 2010). Some of those are inherent to radar-based measurements due to the nature of the measuring technology, but many of them can be addressed using dual-polarimetric data. In Estonia, several filters have been applied to the radar data before it is used in any products. At the signal processor level, speckle and clutter-to-signal ratio filtering is applied. A Doppler filter is used to remove residual non-meteorological fixed clutter. A polarimetric hydrometeor classification-based filter is employed to eliminate non-meteorological targets (Chandrasekar et al., 2013).

The radar scan strategy in Estonia from 2008 to 2020 was based on volume scans with 15-minute intervals (Table 1). While a sufficient number of elevation angles were scanned, the strategy was lacking in repeat time. Low scan intervals did not allow storm tracking and very short-term accumulations. This led to the need for a new scanning strategy, which has been operational since the 18th of May 2020 (Table 2). Since then, full-volume scans have been run every 5 minutes, with the lowest angle repeated every 2.5 minutes. Since the update, the files are

being saved in a sweep-by-sweep manner (each elevation angle as a separate file) instead of all sweeps in one file, which enables even more rapid product generation. All the main scan settings except some filtering are identical and synchronised for both radars, Harku and Sürgavere. This thesis uses only 15-minute interval data from Sürgavere radar to remain uniform.

Table 1. Operational task parameters of Estonian radars from 2008–2020.

Task purpose (type)	Precipitation (PPI)	Doppler wind (PPI)
Elevation angle (°)	0.5/1.5/3/5/7/9/11/15	0.5/1.5/2.5/4/5.5/7/9/11/25
Pulse width (μs)	2	1
PRF (Hz)	570	750/1000
Range (km)	250	130
Output bins	833	866
Bin spacing (km)	0.3	0.15
Samples	42	46
V_{max} (m/s)	7.6	40.0
Repeated (min)	15	15

Table 2. Operational task parameters of Estonian radars since 18.05.2020. Z_{DR} birdbath calibration scan is also run every 15 minutes.

Task purpose (type)	Precipitation (PPI)	Doppler wind (PPI)	Cross section (RHI)
Elevation angle (°)	0.5/1.3/2/3/4.5/6.5/9/0.5	0.5/2/5/(10/15/25/45)	0–60
Pulse width (μs)	1 or 2	0.8	1
PRF (Hz)	570 or 990	900/1200	990
Range (km)	249.9 or 149.9	124	120
Output range bins	833 or 500	620	400
Bin spacing (km)	0.3	0.2	0.3
Samples	32	32	32
V_{max} (m/s)	7.6 or 13.2	48.0	13.2

In order to evaluate and fine-tune radar QPEs, a high-quality gauge network is crucial as a source of reference. Adjusting the radar QPEs with gauge values has become common practice in several countries, and various methods of merging have been developed (Goudenhoofdt and Delobbe, 2009; McKee and Binns, 2016). Recently even a pan-European gauge-adjusted radar precipitation dataset has been produced (Overeem et al., 2022). In Estonia mean field bias method for gauge-radar merging was tested during a project study (Post et al., 2020). Although the results were mixed, a promising framework for future implementation with more advanced adjustment methods and dual-pol data was founded. In this thesis, gauge adjustment is not applied as the focus is solely on comparing various radar products.

2.3 Quantitative precipitation estimation using dual-pol radar

2.3.1 QPE from horizontal reflectivity (ZH)

The classic way to estimate precipitation intensity with a single polarisation weather radar has been through the use of empirical Z–R relationship based on raindrop size distribution in the form of

$$z = AR^b \tag{1}$$

where R is the rainfall rate (mm/h), z is the radar reflectivity factor (mm^6/m^3), and A and b are empirical constants (Rinehart, 1991). More than one hundred Z-R relationships are determined for a specific time, place, and precipitation type. The most commonly used is the one by Marshall and Palmer (Marshall, 1948), where the constants $A = 200$ and $b = 1.6$. In papers II and IV, the following relation by (Joss et al., 1970) was used:

$$z = 300R^{1.5} \tag{2}$$

This relation is chosen to remain equivalent in comparisons in papers II and IV to Italy where it is used (Tiranti et al., 2021) and it is very close also to the one used for rain in Finland (Saltikoff et al., 2015).

It is widely known that QPE based on the horizontal reflectivity of C-band radar is greatly affected by the attenuation of the electromagnetic wave in heavy rain or a wet radome, hail contamination, partial beam blockage and radar absolute calibration (Krajewski et al., 2010; Tabary, 2007). Dual-polarisation technology acquires additional information about the targets through the transmission and reception of horizontally and vertically polarised electromagnetic waves. In operational weather radars, differential propagation phase ϕ_{DP}, specific differential phase K_{DP}, differential reflectivity Z_{DR} and the copolar correlation coefficient ρ_{HV} supply extra information that helps alleviate some issues with horizontal reflectivity-based QPEs.

Differential propagation phase ϕ_{DP} is the relative phase between horizontal and vertical channels. The speed of propagation of the electromagnetic wave is affected by the refractive index of the medium in which it travels. Larger raindrops are more oblate (longer on the horizontal axis than the vertical axis) than small drops. This makes a volume filled with raindrops to have a larger refractive index for horizontally polarised waves than for the vertically polarised one. This causes a slight relative propagation delay for horizontally polarised waves. This leads to a phase difference between horizontal and vertical at low elevation angles. ϕ_{DP} is measured in degrees, and it accumulates along the radar beam. The range derivative of ϕ_{DP} is known as the specific differential phase K_{DP}. It shows the change of phase in degrees per unit distance:

$$K_{DP} = \frac{1}{2}\frac{d\phi_{DP}}{dR}\ [°/\mathrm{km}] \tag{3}$$

where the term $\frac{1}{2}$ accounts for phase shift occurring on the way to the radar bin and back.

The copolar correlation coefficient is a statistical correlation between the reflected horizontal (S_{hh}) and vertical (S_{vv}) power returns and is defined as

$$\rho_{HV} = \frac{\langle S_{vv} S_{hh}^{*} \rangle}{(\langle S_{hh}^{2} \rangle^{1/2} \langle S_{vv}^{2} \rangle^{1/2})} \tag{4}$$

The magnitude of ρ_{HV} is related to the diversity of particle shapes, orientations, and phase states. It is close to 1 in pure rain and generally over 0.9 in precipitation, while it can be from 0.7 to 0.95 in the melting layer (Bringi and Chandrasekar, 2001).

Differential reflectivity Z_{DR} is the ratio of power received in horizontal versus vertical channel:

$$Z_{DR} = 10log_{10}\frac{Z_{hh}}{Z_{vv}}[dB] \tag{5}$$

The larger horizontal axis of raindrops causes the power measured at horizontal polarisation to be larger than the power measured at vertical polarisation. Thus Z_{DR} is generally larger than 1 in the rain.

All radar reflectivity-based applications are subject to Z_H calibration correctness. Both Estonian radars are calibrated per manufacturer instructions once a year with an external signal generator. Still, a bias might be in effect after calibration using this method. In papers II, III and IV, horizontal reflectivity was recalibrated using an approach that makes use of the knowledge that Z_H, Z_{DR}, and K_{DP} are self-consistent with one another, and one can be determined from two of the others. This calibration method is known as self-consistency theory and is explained in detail by (Gorgucci et al., 1992, 1999) and Gourley et al. (2009). The method fundamentally compares the observed differential propagation phase product (ϕ_{DP}^{obs}) to a theoretical differential propagation phase product (ϕ_{DP}^{th}) calculated from Z_H and Z_{DR}. This calibration method requires strict restrictions on the used data discussed in detail in paper II.

2.3.2 QPE from specific differential phase (K_{DP})

Several studies have shown that QPE retrieved from K_{DP} outperforms that of Z_H, especially in heavy rain and is not affected by radar absolute calibration, attenuation or partial beam blockage (Cifelli et al., 2011; Krajewski et al., 2010). However, this field of usage sets high requirements for K_{DP} accuracy. As the K_{DP} in raw data of Estonian radars was found to be of uneven quality, it needed to be

recalculated. For this purpose, the open-source Python ARM Radar Toolkit (Py-ART) was used (Helmus and Collis, 2016). Although the function was available in the toolkit, it needed to be thoroughly tested and fine-tuned as part of the work to obtain results with sufficient quality. The goal to estimate K_{DP} with high accuracy has proven to be a challenge that has been approached by multiple researchers (Giangrande et al., 2013; Lang et al., 2007; Maesaka et al., 2012; Ryzhkov et al., 2005; Schneebeli et al., 2013; Vulpiani et al., 2012). In the last decade, a number of K_{DP} retrieval algorithms have become accessible through open-source software such as Py-ART or Wradlib (Heistermann et al., 2013). While most open-source algorithms are deeply flexible and allow changing various tuning parameters, the implications of changing these parameters often remain unclear. Reimel and Kumjian (2021) were the first to thoroughly compare multiple open-source K_{DP} retrieval algorithms with a focus on the effect of the tuning parameters. They found out that the phase_proc_lp linear programming algorithm (Giangrande et al., 2013) provided in Py-ART was one of the best performers of the seven algorithms they compared as it exhibited the highest versatility. It allowed the production of consistently accurate results in areas with steep K_{DP} gradients and large K_{DP} magnitudes and also in places where K_{DP} gradients were gentler.

The function phase_proc_lp in Py-ART was used in papers II and IV, and it is extensively described in Giangrande et al. (2013). This function offers 12 different user configurable parameters within the Py-ART implementation. Some of the most important of those are:

- Freezing level height ('fzl') – this enables us to define the height in meters at which the 0°C level is located. Any ϕ_{DP} values above this level are not processed because the ϕ_{DP} monotonicity constraint is not applicable in the mixed phase. The default value is 4000 m.
- Minimum Z_H threshold ('low_z') – Low limit for reflectivity in dBZ. Any value below this threshold is set to this limit. The default is set to 10 dBZ.
- Maximum Z_H threshold ('high_z') – High limit for reflectivity in dBZ. Any value above this threshold is set to this limit. This is meant to serve as a cap on Z_H, ensuring that self-consistency between K_{DP} and Z_H is not contaminated by hail. The default value is 53 dBZ.
- Weight of radar self-consistency ('self_const') – This determines how much weight the relationship between Z_H and K_{DP} has in the final solution. The default value is 60 000.
- Self-consistency coefficient ('coef') – It determines the amount of constraint Z_H has on K_{DP}. The default value is 0.914.
- Window length ('window_len') – The length of the Sobel window (number of gates used in the filter window) applied to the ϕ_{DP} field before calculating the final K_{DP} profile. The default value is set to 35.

In papers II and IV, many of those parameters were changed after careful testing with various datasets. The following function in Py-ART was used in paper II to obtain KDP (parameters not written in the function arguments were left with their default values):

pyart.correct.phase_proc_lp(radar, self_const=12000.0, low_z=0.0, high_z=53.0, LP_solver='cylp_mp', proc=15).

In order to calculate the rainfall rate from the recalculated K_{DP}, the following relationship by Leinonen et al. (2012) was used:

$$R = 21.0 K_{DP}^{0.720} \quad (6)$$

Paper II investigates long-term datasets with the aim of obtaining high-quality QPE. Three QPE methods were compared, firstly $R(Z_H)$ using Eq. (1), secondly $R(K_{DP})$ using Eq. (6), and thirdly a combined product $R(Z_H, K_{DP})$. The purpose of the third product, $R(Z_H, K_{DP})$, was to exploit both Z_H and K_{DP} strengths and avoid their shortcomings. Z_H-based QPE is shown to be less accurate in heavy precipitation, while K_{DP}, on the other hand, is noisy in light rainfall (Kumjian, 2013). After testing with various thresholds, the best compromise was found to be such that in the combined method $R(Z_H, K_{DP})$, the $R(Z_H)$ was used when reflectivity was less than or equal to 25 dBZ and $R(K_{DP})$ otherwise.

Extreme precipitation analysis sets even stricter data quality restrictions than long-term accumulation, where some errors are averaged out. Using the phase_proc_lp function with the parameters from paper II for deriving annual 1-hour rainfall maxima led to unrealistically high precipitation amounts and over-smoothed precipitation fields. Therefore the K_{DP} retrieval algorithm needed to be revised for paper IV. After testing with various values of some of the key parameters supported by the findings in Reimel and Kumjian (2021), the function was finally defined as follows:

pyart.correct.phase_proc_lp(radar, self_const = 12000.0, low_z=0.0, high_z=50.0, fzl=3500, LP_solver='cylp_mp', proc=12, window_len=8, coef=0.9).

Notably, the processing window length was reduced from the default 35 to 8, and the self-consistency coefficient from the default 0.914 to 0.9. The decreased window length resulted in increased spatial resolution of the rainfall fields. This was especially beneficial to record small and intense convective rain areas in high quality. Reducing the self-consistency coefficient and the maximum Z_H limit removed the overestimation in high rainfall rate areas contaminated by hail. The same $R(Z_H, K_{DP})$ method from paper II with a 25 dBZ threshold was also used for paper IV.

In addition to the parameters set in the phase_proc_lp function, the data was additionally limited to a 70 km radius from the radar location. Data from the 1st of May until the 30th of September was used. These limitations were set to ensure that radar data originated mainly from liquid precipitation. Five years of radar and rain gauge data from 2011–2018 were used (data from 2014, 2015 and 2017 were excluded due to radar data quality issues) in accumulation analysis.

2.4 Estimation of extreme precipitation and return periods from radar data

In case of heavy rainfall, the precipitation accumulates at a rate which exceeds a criterion specific to the corresponding geographic area. This threshold varies significantly across the globe. In Estonia, multiple definitions of heavy rainfall have been used, from descriptive to specific numeric values. Typically, heavy rainfall has been described as intense rainfall during which water cannot infiltrate into the soil (Tammets et al., 2012). The numeric equivalent used for that has been precipitation of 1 mm or more per 1 minute. Current official thresholds of heavy precipitation used by the Estonian Environment Agency are divided into three classes based on the threat level:

- Level 1 (dangerous): ≥25 mm/12 h or ≥20 mm/1h
- Level 2 (very dangerous): ≥50 mm/12h or ≥30 mm/1h
- Level 3 (extremely dangerous): ≥70 mm/12h or ≥50 mm/1h

None of those is based on a systematic statistical analysis of return periods but is subjectively chosen based on historical data, experience and consultation with neighbouring countries NMS's. Precipitation extremes have commonly been analysed in Estonia in relatively long accumulation periods starting from daily to yearly. Only recently, Olsson et al. (2022) analysed sub-daily rainfall extremes in the Nordic-Baltic region, including data from several rain gauge locations in Estonia. One of the reasons behind the scarcity of short-duration extreme precipitation studies is the lack of high temporal resolution data. Daily maximums have been available from some stations already since 1889, but there is no quality-controlled database of hourly or shorter-period maxima. Nevertheless, it is well known that very intense rainfall does not last very long in Estonia while still causing considerable damage to infrastructure and causing economic losses. Usually, the length of a downpour is no more than 1 hour, and the intensity is highly variable in space and time (Tammets et al., 2012). Considering Estonia's relatively sparse gauge network, many intense rainfall cases have not been recorded in the meteorological database. Even in countries covered by dense gauge networks, most convective storms pass by the gauges. In Germany, only 17.3% of hourly heavy precipitation events (≥25 mm) from 2001 to 2018 were recorded by the gauge network, while nearly 82% of the daily events (≥90 mm)

were captured by the gauges (Lengfeld et al., 2020). Considering that the gauge network in Estonia is nearly 7 times more sparse, then even lower detection efficiency can be expected.

To account for future extremes, engineering design standards are required to adapt to climate change. For a long time, hydrologists and engineers have used return periods and intensity-duration-frequency (IDF) curves to establish such design standards (Martel et al., 2021; Yan et al., 2020). A typical application for such information is the design of city drainage systems (Tamm et al., 2023). To answer a question, for example, can the current drainage systems cope with a rainfall event that occurs, on average, once every 50 years (i.e. the 50 years return level)? Return periods for specific precipitation amounts are estimated by extreme value theory (EVT) (Coles et al., 2001).

Paper IV demonstrates that thanks to the high spatial resolution, even a limited radar time series of 5 years can be used to successfully obtain IDF curves for the climatologically homogeneous area. The basic idea of the utilised method is that the values from the radar annual maxima field can be used as a one long time series if the maxima are statistically independent and are located in the same climatologically homogeneous area. Based on the analysis by Olsson et al. (2022), we can expect a uniform precipitation regime in our study area that is limited to a 70 km range from the radar and includes only continental parts of Estonia. The historical use of statistics of extremes in hydrological and climatological applications dates back to the first half of the 20th century (Gumbel, 1941). Already then, the inherent problem of the statistical estimation of the precipitation return periods was stated that one has to remember when working with such data. It states, in principle, that to apply any theory, we have to suppose that the data are homogeneous, meaning that no systematic change of climate has occurred during the observation period and no such changes will happen in the period for which extrapolations are made (Gumbel, 1941). Because the intensification of the hydrologic cycle, including the increase in the intensity of extreme precipitation events, is anticipated as part of global climate change, this sets limits to this methodology (Tabari, 2020). To mitigate this issue, trends in hydrologic extremes should be incorporated into extreme value analyses. In this thesis, a more straightforward approach has been used in which trends are not considered because the study period needs to be longer for trend estimation.

In paper IV, generalised extreme value distribution (GEV) is used with the method of maximum likelihood (MLE) to estimate the GEV distribution parameters from sample data (Katz et al., 2002). Random samples of annual maxima are expected to be distributed as the GEV cumulative distribution function $F(z)$ (Coles et al., 2001):

$$F(R_{1h} \leq z) = exp\left\{-\left[1 + \xi\left(\frac{z-\mu}{\sigma}\right)\right]^{\frac{-1}{\xi}}\right\} \quad (7)$$

where $R_{1h}$is the random variable of annual maximum rainfall accumulation of one hour and the parameters μ, σ and ξ represent the location, scale, and shape

of the distribution function, respectively. In this work, Gumbel distribution ($\xi = 0$) is assumed for annual rainfall maxima, which is also supported by the findings in Olsson et al. (2022).

Deriving return periods longer than the rainfall record in our study area is justified by assuming constant GEV distribution parameters (Overeem et al., 2010). Nevertheless, the spatial correlation of measurements has to be considered as well because it affects extreme value statistics, causing underestimation (Overeem et al., 2009). In order to mitigate the effect on the extreme value statistics, the measurements should be uncorrelated. Typically for convective precipitation, the area of intense rainfall is in the order of 10 – 100 km^2. Since there is about 1 rain gauge per 1000 km^2 in Estonia, the spatial correlation for gauge measurements is not an issue. Radar data, on the other hand, has a much higher spatial resolution. Depending on the distance from the radar, the resolution of the raw radar data ranges from 0.05 km^2 to 1.3 km^2 (1° × 300 m). Therefore, the correlation between the grid points must be determined and accounted for by resampling the radar data. Semi-variogram analysis is commonly used in geostatistical sciences to estimate precipitation spatial structure (Liu et al., 2018; Phillips et al., 1992; Touma et al., 2018). It is possible to obtain a semi-variogram by taking half the average of the squared difference between data pairs at equal distances and by assuming stationarity and isotropy of the rainfall field (Cressie, 1993):

$$\gamma(h) = \frac{1}{2n(|h|)} \sum_{k=1}^{n(|h|)} (z(x_k + h) - z(x_k))^2 \quad (8)$$

where x_k is the location of cell barycentre k and $x_k + h$ is the location at distance h from location x_k.

Semi-variograms reveal the spatial relations in the data and determine within what range data are spatially autocorrelated (Aalto et al., 2013).

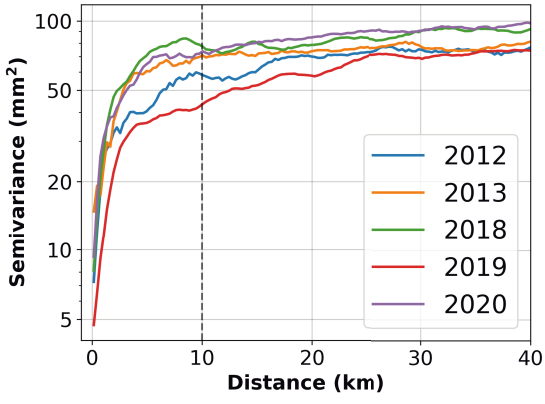

Figure 2. Empirical variogram for hourly rainfall annual maxima based on R(Z_H, K_{DP}) in Estonia. Adapted from paper IV.

Semi-variograms were obtained from annual hourly R(Z_H, K_{DP}) rainfall maxima from 5 years from May to September in paper IV. The results indicated that hourly rainfall maxima decorrelate at about 10 km (Figure 2). This agrees with the typical spatial scale of convective precipitation systems. Thus, the annual hourly rainfall maxima needed to be resampled to the determined spatial scale to avoid statistical oversampling and ensure statistically independent data points. Finally, 93 annual hourly maxima data points from rain gauges and 800 data points from weather radar were used. Then based on these datasets, the statistical analysis and return period estimation was made using the R package ExtRemes 2.1 (Gilleland and Katz, 2016). Annual hourly maxima were derived from the dataset consisting of five years of radar data (2012–2013 and 2018–2020) and ten years of gauge data (2011–2020).

2.5 Estimating lightning and hail from radar data

The electricity of convective storms is strongly related to the convective cell's vertical extent and the updraft's intensity. Many studies have shown that a convective storm becomes electrically active after the ice phase develops (Carey and Rutledge, 1996; Goodman et al., 1988; Workman and Reynolds, 1949). Graupel or hail particles collide with small ice crystals in the turbulent airflow in the convective cloud. These collisions cause the transfer of electric charges between the particles and result in a positively charged cloud top and a negatively charged lower part. Lightning happens when the strength of the charge overpowers the insulating properties of the atmosphere (Dwyer and Uman, 2014).

The oldest systematic records of thunderstorm activity are human observations made at weather stations. The long data series dating back over 100 years at numerous sites is the main advantage of human observations. Otherwise, there are many limitations and disadvantages related to human observations, such as subjectivity and spatiotemporal representativeness. Human observations of lightning have nowadays been primarily superseded by remote sensing, which allows the collection of continuous near real-time data over large areas with high spatiotemporal resolution. Remote sensing of lightning using lightning detectors is based on detecting electromagnetic waves generated by lightning. Lightning detector networks operate in various frequency bands, determining the maximum range, detection efficiency and accuracy. Nordic Lightning Information System (NORDLIS) CG lightning data was used in this work. NORDLIS network consists of about 40 sensors located in Denmark, Estonia, Finland, Latvia, Lithuania, Norway and Sweden. For Finland, it has been found that the first stroke detection efficiency for CG lightning is about 95% (Tuomi and Mäkelä, 2007). The location error of detected CG lightning for most of Estonia and its surrounding areas is between 200–500 m. Lightning detector networks are an accurate source of momentary point measurements indicating the locations of individual strokes. However, they cannot be used to predict where and when lightning might happen. This is where weather radar data, with its gradual nature, can provide additional value.

With weather radar, it is possible to see which cells are growing quickly and approaching the properties required for lightning. It has been shown that the occurrence of the high rate and density of CG flashes is related to the period of the rapid increase in radar echo top height (ET) (Stolzenburg, 1994).

The detection of hail is a more significant challenge than that of lightning. The most extended datasets are also human observations, but they are even more spatiotemporally limited than the ones of lightning. A human can hear lightning up to a distance of 25 km, but hail has to fall in the vicinity of a few hundred meters to be observed (Enno et al., 2013). Moreover, unlike lightning, it is impossible to detect hail directly with any remote sensing instrument. Due to these reasons, the datasets used in hail studies often originate from multiple sources – insurance claims, newspaper reports and, in some cases, hailpad networks (Punge and Kunz, 2016). In recent years, crowdsourcing has also become an important origin (Barras et al., 2019). In the case of this work, none of those was available in the required quality for the Estonian domain. Therefore, we used the proxy data of the hail class from radar hydrometeor classification, which uses dual polarimetry.

Sürgavere radar data from 2011–2014 were used to study lightning and hail estimation products. Only the warm season was considered (May-September), when most of the convective storms occur. Firstly convective precipitation areas were distinguished from the lowest elevation PPI using a 35 dBZ threshold, and then several attributes were calculated for each cell. Altogether 16 attributes (also counting various ET-s) were calculated for each identified cell:

- **Maximum reflectivity**, which indicates the maximum base level PPI reflectivity in the storm cell area
- **Maximum ET height**, defined as the maximum height of a given reflectivity value (0–45 dBZ in 5 dBZ steps) in the storm cell area
- **Storm cell area:** area of a detected polygon with reflectivity exceeding 35 dBZ
- **Maximum lightning activity** within the storm cell (flash/km^2) based on a 1 × 1 km lightning intensity grid generated by counting the CG flashes in a 10 km radius from the grid point centre over 15 min, starting 7.5 min before the nominal scan time
- **Hail top height** which indicates the hydrometeor classification hail maximum height in the cell
- **Graupel top height:** the same as hail top height but for graupel
- **Probability of hail (POH)** in the cell, POH = 0.319 + 0.133ΔH, where ΔH is the 45 dBZ ET difference from the freezing level (Holleman, 2001; Waldvogel et al., 1979). It has been commonly used in operational service, e.g. in Belgium, Finland and The Netherlands (Delobbe and Holleman, 2006, 2003; Saltikoff et al., 2010). In this work freezing level height was acquired from the atmospheric sounding data measured once per day in ESTEA Harku station.

Maximum lightning activity was used only for the general overview of the storms.

In order to find out the potential of each storm cell attribute to indicate lightning or hail, the cells were divided into four types:

- Storms with lightning activity
- Storms without lightning activity
- Storms with hail
- Storms without hail

Then based on this classification, the following events were identified:

a) Success, if the classification correctly indicated lightning/hail activity
b) False alarm, if the classification incorrectly indicated lightning/hail activity
c) Failure, if the cell had lightning/hail, but the classification did not show it
d) Correct negative if the cell did not have lightning/hail and the classification did not show it.

Based on these recorded events, five traditional verification scores were calculated: the probability of detection (POD), false alarm ratio (FAR), critical success index (CSI), equitable threat score (ETS), and Heidke skill score (HSS) (Wilks, 2011).

3 RESULTS AND DISCUSSION

3.1 Convective storms in Estonia 2010–2019

A convective storm is a widespread summertime phenomenon in Estonia. According to the analysis of 9 years summer periods (May, June, July, August, September) in paper III, convective precipitation (reflectivity over 35 dBZ) occurs in 76% of the days in the study area, severe convective storms in 45% of the days and CG lightning flashes in 54% of the days. These results can be compared to the only similar work done in the region by Punkka and Bister (2005). Their study area matched the Finnish weather radar network coverage of the time and consisted of 7 radars that partially covered Estonia. They found that based on the years 2000 and 2001, the fraction of days with convective precipitation (40 dBZ) was 88%, and the fraction of heavy convective precipitation (50 dBZ) was 61%. The higher frequency of occurrence of convective storms found in their study primarily relates to the larger study area of their work. This kind of statistics is undoubtedly somewhat arbitrary. If we extended the study region, the frequency would eventually reach 100%. However, these percentages are helpful for weather forecasters.

The diurnal cycles of convective activity in the Estonian domain are illustrated in Figure 3. It can be seen that all three datasets have a pronounced maximum in the afternoon around 12–13 UTC (15–16 local time). Initial convective cells are more evenly distributed because of the relatively low detection threshold of 35 dBZ (Figure 3a). Severe convective storm cells distribution correlates better with lightning data (Figures 3a and 3b). The difference is lower relative frequency outside the afternoon maximum compared to CG lightning. This can be related to the merging of the storm areas, which reduces the number of detected cells while lightning activity continues or even increases in the remaining cells.

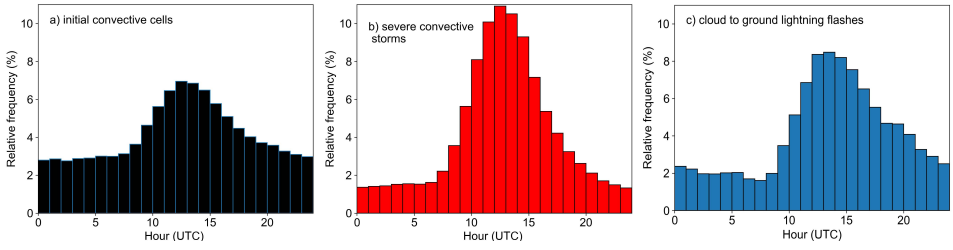

Figure 3. (a) Diurnal cycles of the initial convective cells (35 dBZ reflectivity); (b) severe convective storms (reflectivity ≥ 51 dBZ, CAPE ≥ 80 J/kg); (c) CG lightning. Adapted from paper III.

The spatial distribution of severe convective storms from 2010–2019 (Figure 4) reveals that the most active area is the W and SW part of continental Estonia, with up to 8 storm days per 100 km^2 grid cell per year. It can also be seen that the storm detection efficiency depends on the range from the radar site, and it falls noticeably in further away areas. Considerable falloff starts beyond 100 km from the radar where the centre of the beam of the lowest elevation angle is at the height of 1.7 km, and a single radar bin covers the area of 0.5 km^2. In the West Estonian archipelago, the estimated severe convective days per year range between 2–4 days. Lightning flash density analysis by Enno et al. (2020) using data from 2008–2017 confirms the continental Estonia W and SW part maximum but also shows a second maximum in the hilly SE Estonia which is already off the best working range of the radar and thus not visible in Figure 4.

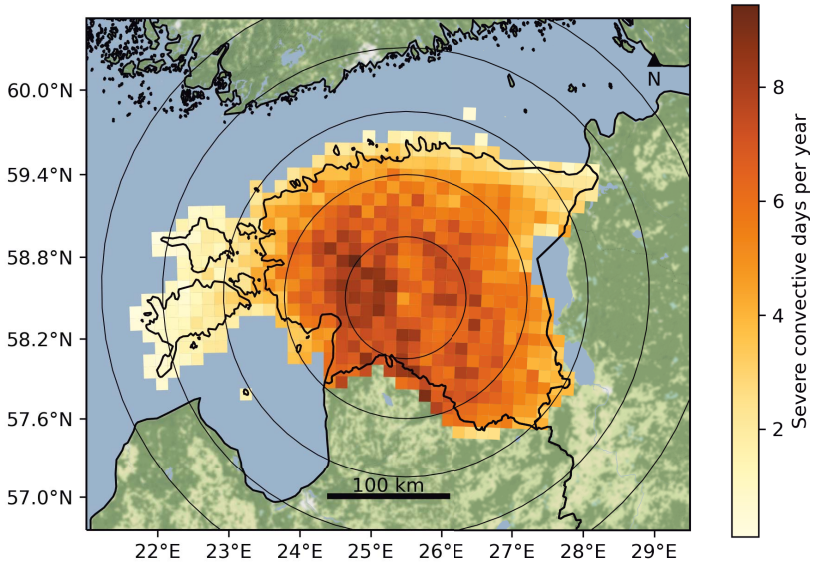

Figure 4. Severe convective storm (reflectivity ≥ 51 dBZ, CAPE ≥ 80 J/kg) days per year on 10 × 10 km grid cells. Black circles centred on the radar location have a step of 50 km. Data from 2010–2019. Adapted from paper III.

It is well known from climatology that the prevailing airflow directions at higher mid-latitudes are westerlies which can be seen in Figure 5a. This also partially explains the spatial distribution of convective storms. Figure 5a confirms that the studied period of 2010–2019 generally represents the longer period well. Nevertheless, compared to the 40-year reference period, the W and SW directions are even more pronounced in our study period, with a slight increase in the E direction. At the same time, the frequency of NW and N flows has decreased. Expectedly, the highest number of convective storms coincide with these directions (Figure 5b). However, the highest probability for a severe convective storm is in the case of SE or S airflow, 62% or 60%, respectively (Figure 5c).

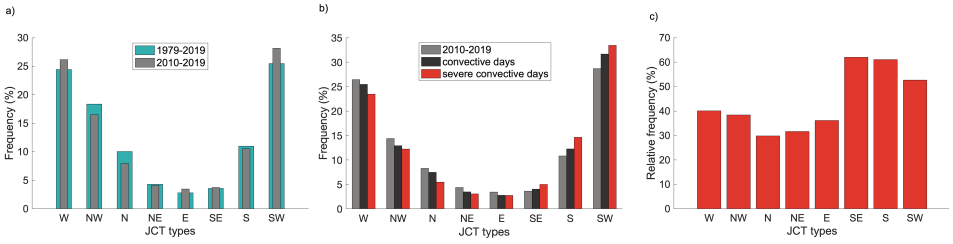

Figure 5. Relative frequency distributions of JCT8 MJJAS 500 hPa types in case of (a) all days in MJJAS 1979–2019 vs 2010–2019; (b) all days in MJJAS, convective days and severe convective days in 2010–2019; (c) probability for a severe convective day during the corresponding JCT. Adapted from paper III.

3.2 Precipitation accumulations

Five years of radar data based precipitation accumulations were compared with the ones from the gauges from the period of 2011–2018. The time series analysis of precipitation accumulation reveals that the correlation between radar QPE products and gauge measurements fluctuates in time (Figure 6). The performance of each QPE algorithm depends on the precipitation intensity, among other factors. The horizontal reflectivity-based product R(Z_H) can estimate rainfall accurately in light rain, where R(K_{DP}) substantially overestimates the amounts. On the other hand, in heavy precipitation (such as on the 21st of June 2016, when 51 mm of rainfall was measured in Tartu-Tõravere station in 2 h), the R(K_{DP}) shows good correlation, and in these situations, the R(Z_H) underestimates rainfall amounts.

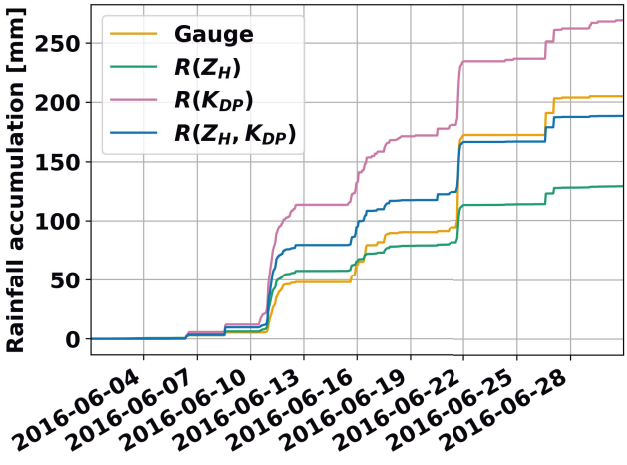

Figure 6. Rainfall cumulative accumulation in 1 h steps for June 2016, three radar data-based QPE products compared to Tartu-Tõravere station gauge data. Z_H is not corrected for attenuation. Adapted from paper II.

The method R(Z_H, K_{DP}), which combines the previous two products using either one's strengths, performs the best, especially over a long period with precipitation events of various intensities. By the end of the 1-month accumulation period, the R(Z_H, K_{DP}) was the closest to the gauge result by underestimating nearly 17 mm (8%), whereas R(K_{DP}) overestimated the reference value by 64 mm (31%) and R(Z_H) underestimated by 76 mm (37%). This can be further validated in more extended data series, including more stations.

The long-term analysis included 5 years of summer (the 1st of May to the 30th of September) data up to 70 km range of the radar and the station data from 8 gauges within that distance limit. The results indicate that the combined method R(Z_H, K_{DP}) outperforms both other methods on all accumulation timescales from 1 hour to 1 month. The longer the compared period, the higher the correlation is with rain gauges. On hourly accumulations (Figure 7), the scatter is higher than on the monthly timescale (Figure 8), partly due to the low 15-minute radar scan interval. The random error caused by a low sampling rate is less relevant on longer accumulation intervals than on shorter ones.

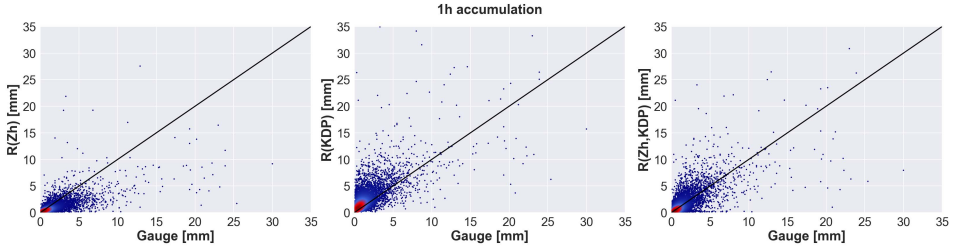

Figure 7. Hourly accumulations for Estonia, 5 years from 2011–2018. Adapted from paper II.

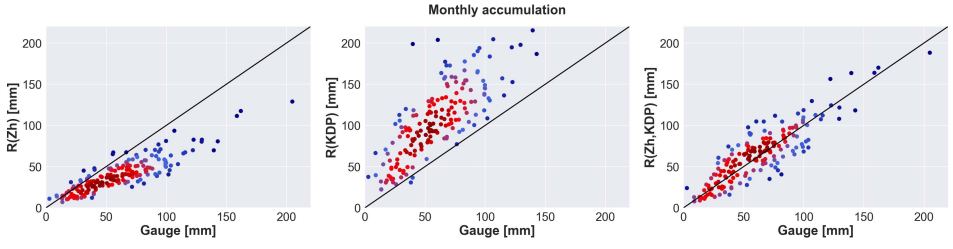

Figure 8. Monthly accumulations for Estonia, 5 years from 2011–2018. Adapted from paper II.

When all accumulation lengths are considered, the $R(Z_H, K_{DP})$ performs the best in almost all verification scores (Table 3). It has the highest Pearson's correlation coefficient (r) of 0.800, Nash-Sutcliffe efficiency (NSE) of 0.354 and lowest normalised mean absolute error (NMAE) of 0.415. A slight overestimation is indicated by the normalised mean bias (NMB) value of 0.250, while for $R(Z_H)$, it is –0.159, and for $R(K_{DP})$, 1.731. All the verification scores improve for every QPE method with increasing accumulation length (except for root mean square

error (RMSE) because longer accumulation lengths naturally bring along higher absolute error). The mean RMSE for $R(Z_H, K_{DP})$ is 7.458 mm, for $R(Z_H)$ 11.143 mm, and for $R(K_{DP})$ 23.931 mm.

Table 3. Mean verification scores of 1-hour, 24-hour and monthly accumulations from 5 years of data 2011–2018.

	$R(Z_H)$	$R(K_{DP})$	$R(Z_H, K_{DP})$
r	0.796	0.752	0.800
NMAE	0.457	0.845	0.415
NMB	–0.159	1.731	0.250
RMSE (mm)	11.143	23.931	7.458
NSE	0.235	–0.353	0.354

3.3 Extreme precipitation analysis and return periods

IDF curves have been developed before in many studies from horizontal reflectivity (Marra et al., 2017; Marra and Morin, 2015; Overeem et al., 2010; Saltikoff et al., 2019). In paper IV, for the first time, the return intensities from dual-polarisation weather radar are developed from five years of data. The data are derived from operational radar without any dedicated settings and QPEs are obtained without any rain gauges adjustment. Figure 9 shows the return intensities for hourly rainfall at a given return time. The general agreement between gauges and radar $R(Z_H, K_{DP})$ QPE is good, with gauges estimating generally smaller return intensities on all return periods. The return intensities of $R(Z_H, K_{DP})$ are 14–19% higher than the return intensities of gauges. The uncertainty of the estimates increases in higher intensities, especially for gauge-based values. The different sample sizes determine this: the dataset derived from five years of radar measurements contains 800 values, while the sample size obtained by rain gauges is about nine times smaller. Return intensities based on $R(Z_H)$ are underestimated compared to $R(Z_H, K_{DP})$ being potentially caused by several weaknesses of the $R(Z_H)$ like attenuation in heavy rainfall, partial beam-filling, inappropriate drop size distribution assumed in the Z-R relationship and clutter. Furthermore, the unrealistically large scale parameter and a low statistical significance of the fit indicate low reliability of the return intensities based on $R(Z_H)$.

The differences between gauges and radar can stem from multiform factors – in addition to different measurement locations, and representative area radar provides temporal snapshots of the rainfall and, thus, contrary to the gauges, does not provide temporal integrals. Extreme precipitation tends to be highly variable in space and time, resulting in different effects on radar and gauge data. All these factors affect the distributional properties, and the proper quantification of these effects is complicated.

The radar QPE-based return levels shown in Figure 9 can be compared to the official precipitation warning thresholds used by the Estonian Environment Agency to estimate how often each threshold might be exceeded in the territory of Estonia:

- Level 1 (20 mm/1h) – once per 2 years
- Level 2 (30 mm/1h) – once per 10 years
- Level 3 (50 mm/1h) – once per more than 100 years.

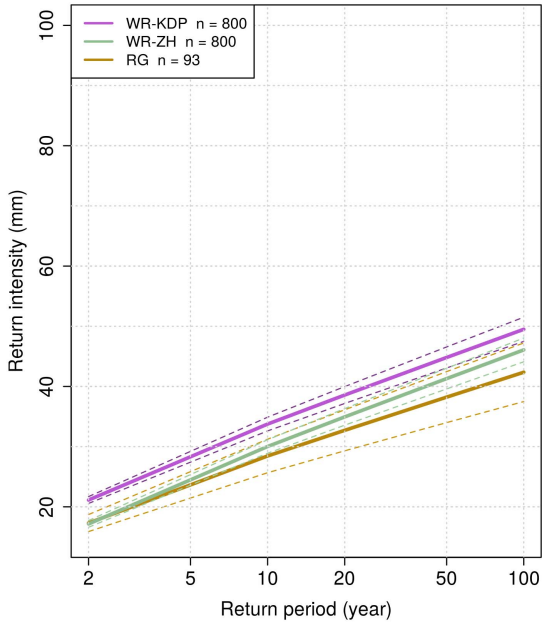

Figure 9. Return intensities of 1-hour rainfall based on $R(Z_H, K_{DP})$, $R(Z_H)$ and rain gauges. The dashed lines denote confidence intervals for α = 0.05. Adapted from paper IV.

These results are likely valid for any point in continental Estonia. At the same time, the return intensities for coastal areas and islands are expected to be lower due to lower precipitation amounts in these regions. Because of the distance limitation of the radar QPE, current weather radar network coverage does not allow quantifying these expectations. More radar sites with high-quality long-term datasets are required to apply these methods in all Estonian areas. This study is also limited to a warm period since $R(K_{DP})$ works reliably only in liquid water. Nevertheless, this is not an issue because only 1-hour accumulation maxima are considered here, and it has been shown that these occur in the region only in the summer from June to September (Olsson et al., 2022). Regardless of the limited availability of the radar time series of just five years, the results are in good agreement with studies from the same region using more extended datasets of only gauge data (Olsson et al., 2022). This encourages further studies using the same methodology with shorter accumulation lengths in the future when the high temporal resolution dataset of sufficient length becomes available.

3.4 Lightning and hail

Lightning and hail in convective storms were studied based on 4 years of data. A total of 123 360 individual convective cells were derived using a 35 dBZ threshold. Of these cells, 33.9% included lightning, and 25.9% included hail. These percentages could be considered the prior probabilities of these phenomena using the set reflectivity threshold. The performance and added value of the storm cell attributes to detect lightning onset can be analysed based on the comparison of skill scores shown in Figure 10.

For lightning estimation, echo tops showed the best results. Hail and graupel height skill scores showed uneven performance and did not outscore the best echo tops in any category. ET15 and ET20 have the highest CSI value of 0.39. ET20 and ET25 are the best in terms of HSS (0.26 and 0.27, respectively) and ETS (0.15 and 0.16). When comparing the POD scores, it can be seen that the higher the ET threshold, the lower the POD. One of the reasons behind this is partly the convective cell definition of 35 dBZ which means that a number of storms do not have reflectivities exceeding higher values. The good distinction between lightning and non-lightning storm areas of echo top products is also visible from the histograms in Figure 11. Especially ET20 has distinctive distributions for both types of storms. Generally, the differences between several echo top attributes maximum CSI, HSS and ETS are small, and therefore it depends on the user's preferences for which characteristics to prioritise. ET15, ET20 and ET25 were all very similar among those skill scores. If the priority were low FAR, ET25 would be most suitable. However, if high POD were the most important, ET15 would be preferable. Therefore ET20 could be considered the optimal choice as its scores are in the middle.

Hail from the polarimetric hydrometeor classification was compared with maximum reflectivity and probability of hail (POH) from the 35 dBZ convective storm cells. The skill scores for the maximum reflectivity as hail estimator reach maximum values just below 50 dBZ with HSS around 0.6, FAR around 0.3 and POD around 0.8 (Figure 12a). Somewhat unexpectedly, POH scores were lower and reached their maximum already at a POH value of 0.2, where HSS and FAR were around 0.48 and POD around 0.8 (Figure 12b). From the equation used to calculate the POH values, it appears that to obtain POH > 0, the reflectivity needs to exceed 45 dBZ, and the height difference ΔH needs to be greater than –2.4 km. As seen from the histogram in Figure 13a, hail can occur in cells with maximum reflectivity starting from 40 dBZ, which already decreases the detection efficiency of the POH algorithm. It has been found that POH might be too restrictive in identifying hail areas by a study comparing it to hail reports, suggesting that using a lower reflectivity threshold in the algorithm should be considered (Barras et al., 2019). The required height difference could also need to be revised for Estonian data because of climatological differences. Therefore, although based on our study of these two hail estimators, maximum reflectivity of 50 dBZ is the best, additional testing and tuning of the POH parameters could increase the performance of this algorithm in Estonia as well.

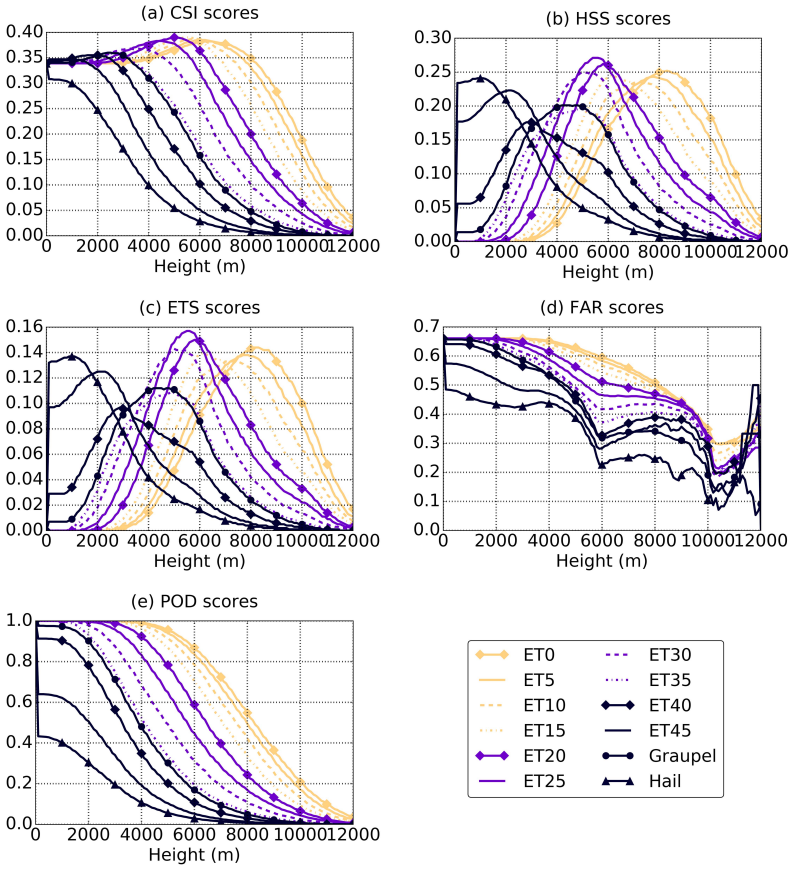

Figure 10. Skill scores (CSI – critical success index, HSS – Heidke skill score, ETS – equitable threat score, FAR – false alarm rato, POD – the probability of detection) as a function of classification threshold for ET0-ET45, hail altitude and graupel altitude as cloud-to-ground lightning indicators. Adapted from paper I.

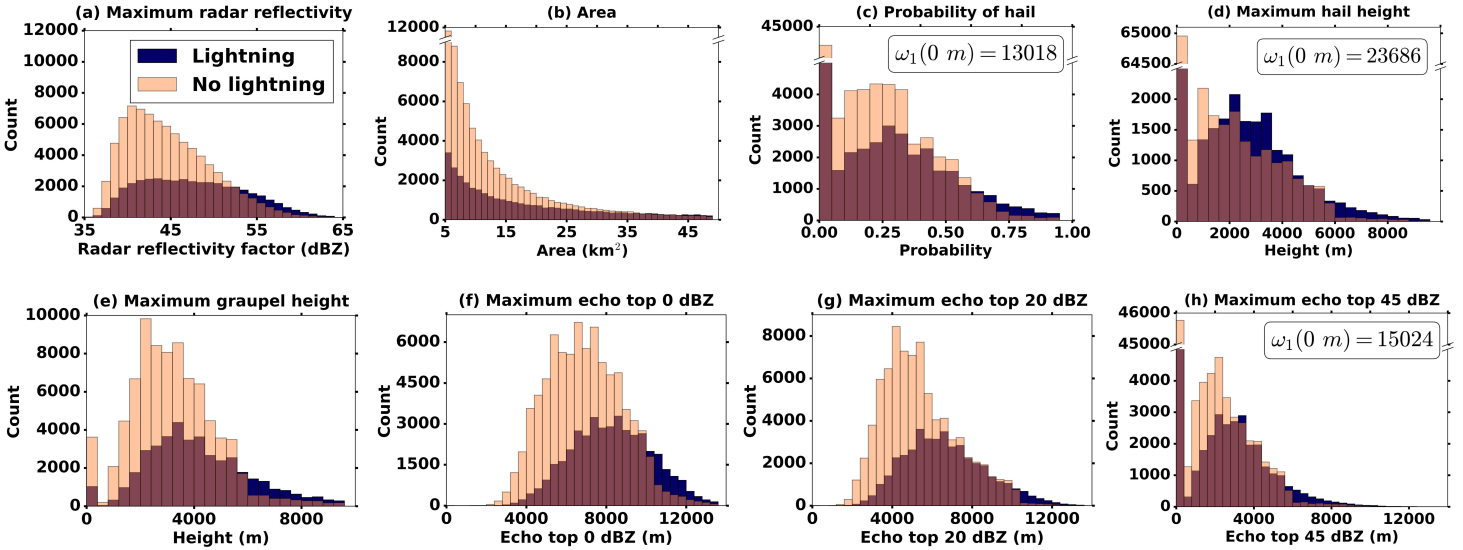

Figure 11. Histograms of (a) cell maximum reflectivity; (b) cell area; (c) probability of hail; (d) hail height; (e) graupel height; (f) ET0; (g) ET20; (h) ET45 divided to classes of storms with lightning activity (ω_1) and storms without lightning activity (ω_2). Adapted from paper I.

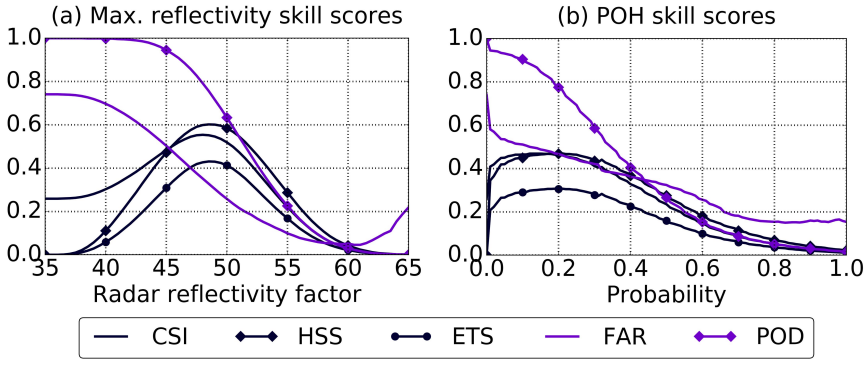

Figure 12. Skill scores (CSI – critical success index, HSS – Heidke skill score, ETS – equitable threat score, FAR – false alarm rato, POD – the probability of detection) as a function of classification threshold for (a) maximum reflectivity and (b) probability of hail (POH) as hydrometeor classification algorithm hail indicators. Adapted from paper I

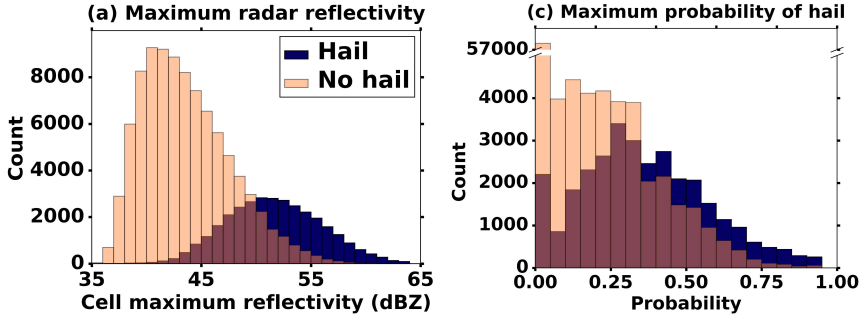

Figure 13. Histograms of (a) cell maximum reflectivity and (b) probability of hail divided into classes of storms with hydrometeor classification algorithm hail (ω_3) and without hail(ω_4). Adapted from paper I.

4 CONCLUSIONS AND OUTLOOK

This thesis shows that using dual-polarisation weather radar can increase the accuracy of estimating severe summertime weather phenomena. One of the most important advantages over the related works in the field is the usage of long-term dual-polarisation radar datasets on which all the data processing algorithms are applied. This helps to obtain robust and reliable results and conclusions. Another practical aspect of this thesis is the usage of data from operational sources and the application of open-source software and algorithms, which ensures a straightforward introduction of the results to operational services and future research.

The radar QPE-related parts of this thesis focused on retrieving the high quality of dual-polarimetric variables and producing long-term precipitation accumulations based comparisons with horizontal reflectivity with minimal additional filtering and adjustment. Three radar QPE products were compared to rain gauge data over the period of 5 years' warm seasons in paper II. The QPE product, which combines horizontal reflectivity with specific differential phase, showed the best correlation with rain gauge data (Pearson's correlation coefficient of 0.800). This combined product utilised the benefits of each individual method and was therefore accurate in both low and high precipitation cases. These QPE products were used further in paper IV, where short-duration extreme precipitation accumulations of 1-hour maxima were analysed. This paper also highlighted the importance of data quality since even a few erroneous data points can infest extreme value statistics. This led to the need to improve the K_{DP} retrieval algorithm parameters in paper IV compared to paper II. The resulting IDF curves demonstrated that polarimetric radar QPE is suitable for extreme precipitation applications. Even from 5 years of radar data, return intensities can be found for up to 100 years, considering the increasing uncertainty. Prerequisite for this being homogeneous precipitation climatology in the region. These findings can be used in hydrological applications and help put the current precipitation warning levels in Estonia into the perspective of occurrence frequency.

Convective storms that include heavy rainfall and other hazardous phenomena, such as lightning and hail, were studied using an automated detection method in papers I and III. Severe convective storm definition (≥51 dBZ reflectivity and ≥80 J/kg CAPE) is proposed in paper III after analysis of various reflectivity levels and NWP model outputs. Significantly, this study, based on 9 years of data, indicates that the highest probability of a severe convective storm is in the case of SE (62%) and S (60%) airflow. In contrast, the most common airflow direction during the period was expectedly from W and SW. Although there is a severe convective storm somewhere in Estonia in almost half of the days (45%) from May to September, and CG lightning is even more frequent (54% of those days), some regions stand out. The most active area in these terms is central continental Estonia, especially W and SW parts (up to 8 storm days per year in a 100 km^2 grid box). In contrast, the least storms occur in the West Estonian archipelago (2 storm days per year in a 100 km^2 grid box). Areas further than 100 km from the radar location

stand out in general by fewer detected storms referring to poor radar coverage. In order to find the best radar-based parameter for lightning and hail onset, the threshold for convective storm area was defined as 35 dBZ in paper I. The threshold was chosen low enough to include also weaker storms. Of these areas, 33.9% included lightning and 25.9% hail. These values can then be considered the prior probabilities of either phenomenon if the reflectivity exceeds 35 dBZ. From the total of 16 different parameters, the best CG lightning indicator was found to be 20 dBZ echo top height and for hail maximum reflectivity.

Most of the results of this thesis have great practical value and could be put into operational use in convective storm detection and nowcasting systems. Nevertheless, there are ways to further improve on the findings of this thesis in the future. Regarding radar QPE, the combined method $R(Z_H, K_{DP})$ could be optimised first by finding a more appropriate threshold based on longer reference period and fine-tuning K_{DP} retrieval method. Precipitation accumulation datasets could be developed further by additional filtering (e.g. by statistical filters and satellite data), and also by gauge adjustment methods like local mean-field bias (Overeem et al., 2022). Several filtering and adjustment methods are available for free in open-source radar data processing software packages such as py-ART or wradlib (Heistermann et al., 2013; Helmus and Collis, 2016). The convective storm analysis could be further developed by introducing cell tracking, enabled by more frequent scanning of up to 2.5 minutes of the lowest level PPI or 5 minutes of full volume scans available from May 2020. The high sampling frequency also enables obtaining reliable return periods of accumulation lengths of less than 1 h. In order to provide high accuracy of those solutions in the whole country, the instrumentation network also needs development. In the current thesis, the radar QPE study area was limited to 70 km from the radar location to obtain data from liquid phase precipitation. Although there are a total of two operational weather radars currently in Estonia, even if we used both, still large areas would remain uncovered. This implies that at least 3 additional radars are needed to cover at least 90% of the land. Sub-hourly precipitation accumulation analysis would benefit also from higher sampling rate of the rain gauge data than the current 10 minute interval to remain comparable with the 5 minute (or 2.5 minute for the lowest elevation) interval of radar scans. In order to perform valid bias adjustment, a sufficient amount of rain gauges are also needed. It has been shown that at least 10–20 gauges are required for that in the 70 km radius from the radar site (Thorndahl et al., 2014). In the current study area there were 8 gauges available in the 70 km radius and there are regions with even more sparse placement of gauges. Therefore the number of gauge measurement sites needs to increase as well.

REFERENCES

Aalto, J., Pirinen, P., Heikkinen, J., Venäläinen, A., 2013. Spatial interpolation of monthly climate data for Finland: comparing the performance of kriging and generalized additive models. Theor Appl Climatol 112, 99–111. https://doi.org/10.1007/s00704-012-0716-9

Alber, R., Jaagus, J., Oja, P., 2015. Diurnal cycle of precipitation in Estonia. Estonian Journal of Earth Sciences 64, 305–313.

Avotniece, Z., 2010. Trends in the frequency of extreme climate events in Latvia Zanita Avotniece, Valery Rodinov, Lita Lizuma, Agrita Briede, Māris Kļaviņš. Baltica 23, 135–148.

Barras, H., Hering, A., Martynov, A., Noti, P.-A., Germann, U., Martius, O., 2019. Experiences with> 50,000 crowdsourced hail reports in Switzerland. Bulletin of the American Meteorological Society 100, 1429–1440.

Bieringer, P., Ray, P.S., 1996. A Comparison of Tornado Warning Lead Times with and without NEXRAD Doppler Radar. Weather and Forecasting 11, 47–52. https://doi.org/10.1175/1520-0434(1996)011<0047:ACOTWL>2.0.CO;2

Bringi, V.N., Chandrasekar, V., 2001. Polarimetric Doppler Weather Radar: Principles and Applications. Cambridge University Press.

Brooks, H.E., Iii, C.A.D., Zhang, X., Chernokulsky, A.M.A., Tochimoto, E., Hanstrum, B., Nascimento, E. de L., Sills, D.M.L., Antonescu, B., Barrett, B., 2019. A Century of Progress in Severe Convective Storm Research and Forecasting. Meteorological Monographs 59, 18.1–18.41. https://doi.org/10.1175/AMSMONOGRAPHS-D-18-0026.1

Brooks, H.E., Marsh, P.T., Kowaleski, A.M., Groenemeijer, P., Thompson, T.E., Schwartz, C.S., Shafer, C.M., Kolodziej, A., Dahl, N., Buckey, D., 2011. Evaluation of European Storm Forecast Experiment (ESTOFEX) forecasts. Atmospheric Research, 5th European Conference on Severe Storms 100, 538–546. https://doi.org/10.1016/j.atmosres.2010.09.004

Browning, K.A., Blyth, A.M., Clark, P.A., Corsmeier, U., Morcrette, C.J., Agnew, J.L., Ballard, S.P., Bamber, D., Barthlott, C., Bennett, L.J., Beswick, K.M., Bitter, M., Bozier, K.E., Brooks, B.J., Collier, C.G., Davies, F., Deny, B., Dixon, M.A., Feuerle, T., Forbes, R.M., Gaffard, C., Gray, M.D., Hankers, R., Hewison, T.J., Kalthoff, N., Khodayar, S., Kohler, M., Kottmeier, C., Kraut, S., Kunz, M., Ladd, D.N., Lean, H.W., Lenfant, J., Li, Z., Marsham, J., McGregor, J., Mobbs, S.D., Nicol, J., Norton, E., Parker, D.J., Perry, F., Ramatschi, M., Ricketts, H.M.A., Roberts, N.M., Russell, A., Schulz, H., Slack, E.C., Vaughan, G., Waight, J., Wareing, D.P., Watson, R.J., Webb, A.R., Wieser, A., 2007. The Convective Storm Initiation Project. Bulletin of the American Meteorological Society 88, 1939–1956. https://doi.org/10.1175/BAMS-88-12-1939

Carey, L.D., Rutledge, S.A., 1996. A multiparameter radar case study of the microphysical and kinematic evolution of a lightning producing storm. Meteorology and Atmospheric Physics 59, 33–64.

Chandrasekar, V., Keränen, R., Lim, S., Moisseev, D., 2013. Recent advances in classification of observations from dual polarization weather radars. Atmospheric Research, Advances in Precipitation Science 119, 97–111. https://doi.org/10.1016/j.atmosres.2011.08.014

Chisholm, A.J., Renick, J.H., 1972. The kinematics of multicell and supercell Alberta hailstorms. Alberta Hail Studies, 1972 24–31.

Cifelli, R., Chandrasekar, V., Lim, S., Kennedy, P.C., Wang, Y., Rutledge, S.A., 2011. A new dual-polarization radar rainfall algorithm: Application in Colorado precipitation events. Journal of Atmospheric and Oceanic Technology 28, 352–364.

Coles, S., Bawa, J., Trenner, L., Dorazio, P., 2001. An introduction to statistical modeling of extreme values. Springer.

Collis, S., Protat, A., May, P.T., Williams, C., 2013. Statistics of Storm Updraft Velocities from TWP-ICE Including Verification with Profiling Measurements. Journal of Applied Meteorology and Climatology 52, 1909–1922. https://doi.org/10.1175/JAMC-D-12-0230.1

Cressie, N.A., 1993. Statistics for spatial data. John Willy and Sons. Inc., New York 800.

Davies-Jones, R., Wood, V.T., Rasmussen, E.N., 2020. Doppler Circulation as a Fairly Range-Insensitive Far-Field Tornado Detection and Precursor Parameter. Journal of Atmospheric and Oceanic Technology 37, 1117–1133. https://doi.org/10.1175/JTECH-D-19-0116.1

Delobbe, L., Holleman, I., 2006. Uncertainties in radar echo top heights used for hail detection. Meteorological Applications 13, 361–374.

Delobbe, L., Holleman, I., 2003. Radar-based hail detection: Impact of height assignment errors on the measured vertical profiles of reflectivity.

Doswell, C.A., 2015. Severe convective storms in the European societal context. Atmospheric Research 158–159, 210–215. https://doi.org/10.1016/j.atmosres.2014.08.007

Ducrocq, V., Tzanos, D., Sénési, S., 1998. Diagnostic tools using a mesoscale NWP model for the early warning of convection. Meteorological Applications 5, 329–349. https://doi.org/10.1017/S1350482798000917

Durage, S.W., Wirasinghe, S.C., Ruwanpura, J., 2013. Comparison of the Canadian and US tornado detection and warning systems. Nat Hazards 66, 117–137. https://doi.org/10.1007/s11069-012-0168-7

Dwyer, J.R., Uman, M.A., 2014. The physics of lightning. Physics Reports, The Physics of Lightning 534, 147–241. https://doi.org/10.1016/j.physrep.2013.09.004

Enno, S.E., Briede, A., Valiukas, D., 2013. Climatology of thunderstorms in the Baltic countries, 1951–2000. Theor Appl Climatol 111, 309–325. https://doi.org/10.1007/s00704-012-0666-2

Enno, S.-E., Sugier, J., Alber, R., Seltzer, M., 2020. Lightning flash density in Europe based on 10 years of ATDnet data. Atmospheric Research 235, 104769. https://doi.org/10.1016/j.atmosres.2019.104769

European Storm Forecast Experiment – ESTOFEX [WWW Document], n.d. URL https://www.estofex.org/ (accessed 10.1.21).

Fallah, A., O, S., Orth, R., 2020. Climate-dependent propagation of precipitation uncertainty into the water cycle. Hydrology and Earth System Sciences 24, 3725–3735. https://doi.org/10.5194/hess-24-3725-2020

Giangrande, S.E., McGraw, R., Lei, L., 2013. An application of linear programming to polarimetric radar differential phase processing. Journal of Atmospheric and Oceanic Technology 30, 1716–1729.

Gilleland, E., Katz, R.W., 2016. extRemes 2.0: an extreme value analysis package in R. Journal of Statistical Software 72, 1–39.

Goodman, S.J., Buechler, D.E., Wright, P.D., Rust, W.D., 1988. Lightning and precipitation history of a microburst-producing storm. Geophysical research letters 15, 1185–1188.

Gorgucci, E., Scarchilli, G., Chandrasekar, V., 1999. A procedure to calibrate multiparameter weather radar using properties of the rain medium. IEEE Transactions on Geoscience and Remote Sensing 37, 269–276.
Gorgucci, E., Scarchilli, G., Chandrasekar, V., 1992. Calibration of radars using polarimetric techniques. IEEE transactions on geoscience and remote sensing 30, 853–858.
Goudenhoofdt, E., Delobbe, L., 2013. Statistical Characteristics of Convective Storms in Belgium Derived from Volumetric Weather Radar Observations. Journal of Applied Meteorology and Climatology 52, 918–934. https://doi.org/10.1175/JAMC-D-12-079.1
Goudenhoofdt, E., Delobbe, L., 2009. Evaluation of radar-gauge merging methods for quantitative precipitation estimates. Hydrology and Earth System Sciences 13, 195–203.
Gourley, J.J., Illingworth, A.J., Tabary, P., 2009. Absolute calibration of radar reflectivity using redundancy of the polarization observations and implied constraints on drop shapes. Journal of Atmospheric and Oceanic Technology 26, 689–703.
Groenemeijer, P., Púčik, T., Holzer, A.M., Antonescu, B., Riemann-Campe, K., Schultz, D.M., Kühne, T., Feuerstein, B., Brooks, H.E., Doswell, C.A., Koppert, H. J., Sausen, R., 2017. Severe Convective Storms in Europe: Ten Years of Research and Education at the European Severe Storms Laboratory. Bulletin of the American Meteorological Society 98, 2641–2651. https://doi.org/10.1175/BAMS-D-16-0067.1
Gumbel, E.J., 1941. The return period of flood flows. The annals of mathematical statistics 12, 163–190.
Heistermann, M., Jacobi, S., Pfaff, T., 2013. An open source library for processing weather radar data (wradlib). Hydrology and Earth System Sciences 17, 863–871.
Helmus, J.J., Collis, S.M., 2016. The Python ARM Radar Toolkit (Py-ART), a library for working with weather radar data in the Python programming language. Journal of Open Research Software 4. https://doi.org/10.5334/jors.119
Hintz, K.S., McNicholas, C., Randriamampianina, R., Williams, H.T.P., Macpherson, B., Mittermaier, M., Onvlee-Hooimeijer, J., Szintai, B., 2021. Crowd-sourced observations for short-range numerical weather prediction: Report from EWGLAM/SRNWP Meeting 2019. Atmospheric Science Letters 22, e1031. https://doi.org/10.1002/asl.1031
Holleman, I., 2001. Hail detection using single-polarization radar. Citeseer.
IPCC, 2021. Climate Change 2021: The Physical Science Basis. Contribution of Working Group I to the Sixth Assessment Report of the Intergovernmental Panel on Climate Change.
IPCC, A., 2014. IPCC Fifth Assessment Report—Synthesis Report. IPCC New York, NY, USA.
Joss, J., Schram, K., Thams, J.C., Waldvogel, A., 1970. On the Quantitative Determination of Precipitation by a Radar. Osservatorio Ticinese Della Centrale Meteorologica Svizzera Locarno-Monti.
Kallis, A., Rosin, K., Pärnpuu, P., Loodla, K., Šišova, V., Ala, T. (Eds.), 2019. 100 aastat Eesti ilma(teenistust). Keskkonnaagentuur, Tallinn.
Katz, R.W., Parlange, M.B., Naveau, P., 2002. Statistics of extremes in hydrology. Advances in water resources 25, 1287–1304.
Kiitsak, K., 2020. Ohtlikud ilmanähtused Eestis 1997–2019 (Thesis). Tartu Ülikool.
Krajewski, W.F., Villarini, G., Smith, J.A., 2010. Radar-rainfall uncertainties: Where are we after thirty years of effort? Bulletin of the American Meteorological Society 91, 87–94.

Kumjian, M., 2013. Principles and applications of dual-polarization weather radar. Part I: Description of the polarimetric radar variables. J. Operational Meteor. 1, 226–242. https://doi.org/10.15191/nwajom.2013.0119

Kyznarová, H., Novák, P., 2009. CELLTRACK — Convective cell tracking algorithm and its use for deriving life cycle characteristics. Atmospheric Research, 4th European Conference on Severe Storms 93, 317–327. https://doi.org/10.1016/j.atmosres.2008.09.019

Lang, T.J., Ahijevych, D.A., Nesbitt, S.W., Carbone, R.E., Rutledge, S.A., Cifelli, R., 2007. Radar-observed characteristics of precipitating systems during NAME 2004. Journal of climate 20, 1713–1733.

Leinonen, J., Moisseev, D., Leskinen, M., Petersen, W.A., 2012. A climatology of disdrometer measurements of rainfall in Finland over five years with implications for global radar observations. Journal of Applied Meteorology and Climatology 51, 392–404.

Lengfeld, K., Kirstetter, P.-E., Fowler, H.J., Yu, J., Becker, A., Flamig, Z., Gourley, J., 2020. Use of radar data for characterizing extreme precipitation at fine scales and short durations. Environmental Research Letters 15, 085003.

Li, Z., Chen, M., Gao, S., Hong, Z., Tang, G., Wen, Y., Gourley, J.J., Hong, Y., 2020. Cross-Examination of Similarity, Difference and Deficiency of Gauge, Radar and Satellite Precipitation Measuring Uncertainties for Extreme Events Using Conventional Metrics and Multiplicative Triple Collocation. Remote Sensing 12, 1258. https://doi.org/10.3390/rs12081258

Liu, D., Zhao, Q., Guo, S., Liu, P., Xiong, L., Yu, X., Zou, H., Zeng, Y., Wang, Z., 2018. Variability of spatial patterns of autocorrelation and heterogeneity embedded in precipitation. Hydrology Research 50, 215–230. https://doi.org/10.2166/nh.2018.054

Maesaka, T., Iwanami, K., Maki, M., 2012. Non-negative KDP estimation by monotone increasing ΦDP assumption below melting layer, in: Extended Abstracts, Seventh European Conf. on Radar in Meteorology and Hydrology.

Marra, F., Morin, E., 2015. Use of radar QPE for the derivation of Intensity–Duration–Frequency curves in a range of climatic regimes. Journal of hydrology 531, 427–440.

Marra, F., Morin, E., Peleg, N., Mei, Y., Anagnostou, E.N., 2017. Intensity–duration–frequency curves from remote sensing rainfall estimates: comparing satellite and weather radar over the eastern Mediterranean. Hydrology and Earth System Sciences 21, 2389–2404.

Marshall, J.S., 1948. The distribution of raindrops with size. J. meteor. 5, 165–166.

Martel, J.-L., Brissette, F.P., Lucas-Picher, P., Troin, M., Arsenault, R., 2021. Climate change and rainfall intensity–duration–frequency curves: Overview of science and guidelines for adaptation. Journal of Hydrologic Engineering 26, 03121001.

McKee, J.L., Binns, A.D., 2016. A review of gauge–radar merging methods for quantitative precipitation estimation in hydrology. Canadian Water Resources Journal/ Revue canadienne des ressources hydriques 41, 186–203.

Meischner, P., 2005. Weather Radar: Principles and Advanced Applications. Springer Science & Business Media.

Nemeth, K., 2008. OTT Pluvio2: Weighing precipitation gauge and advances in precipitation measurement technology, in: WMO Technical Conf. on Meteorological and Environmental Instruments and Methods of Observation.

Olsson, J., Dyrrdal, A.V., Médus, E., Södling, J., Aņiskeviča, S., Arnbjerg-Nielsen, K., Førland, E., Mačiulytė, V., Mäkelä, A., Post, P., Thorndahl, S.L., Wern, L., 2022. Sub-daily rainfall extremes in the Nordic–Baltic region. Hydrology Research 53, 807–824. https://doi.org/10.2166/nh.2022.119

Overeem, A., Buishand, T.A., Holleman, I., 2009. Extreme rainfall analysis and estimation of depth-duration-frequency curves using weather radar. Water resources research 45.

Overeem, A., Buishand, T.A., Holleman, I., Uijlenhoet, R., 2010. Extreme value modeling of areal rainfall from weather radar. Water Resources Research 46.

Overeem, A., van den Besselaar, E., van der Schrier, G., Meirink, J.F., van der Plas, E., Leijnse, H., 2022. EURADCLIM: The European climatological high-resolution gauge-adjusted radar precipitation dataset. Earth System Science Data Discussions 1–34.

Peter, J.R., Manton, M.J., Potts, R.J., May, P.T., Collis, S.M., Wilson, L., 2015. Radar-Derived Statistics of Convective Storms in Southeast Queensland. Journal of Applied Meteorology and Climatology 54, 1985–2008. https://doi.org/10.1175/JAMC-D-13-0347.1

Phillips, D.L., Dolph, J., Marks, D., 1992. A comparison of geostatistical procedures for spatial analysis of precipitation in mountainous terrain. Agricultural and Forest Meteorology 58, 119–141. https://doi.org/10.1016/0168-1923(92)90114-J

Polger, P.D., Goldsmith, B.S., Przywarty, R.C., Bocchieri, J.R., 1994. National Weather Service Warning Performance Based on the WSR-88D. Bulletin of the American Meteorological Society 75, 203–214. https://doi.org/10.1175/1520-0477(1994)075<0203:NWSWPB>2.0.CO;2

Post, P., Toll, V., Rahu, J., Voormansik, T., 2020. Täppissademed.

Punge, H.J., Kunz, M., 2016. Hail observations and hailstorm characteristics in Europe: A review. Atmospheric Research 176, 159–184.

Punkka, A.-J., Bister, M., 2005. Occurrence of summertime convective precipitation and mesoscale convective systems in Finland during 2000–01. Monthly weather review 133, 362–373.

Reimel, K.J., Kumjian, M., 2021. Evaluation of K DP estimation algorithm performance in rain using a known-truth framework. Journal of Atmospheric and Oceanic Technology 38, 587–605.

Rinehart, R.E., 1991. Radar for meteorologists. University of North Dakota, Office of the President.

Rossi, P.J., Hasu, V., Koistinen, J., Moisseev, D., Mäkelä, A., Saltikoff, E., 2014. Analysis of a statistically initialized fuzzy logic scheme for classifying the severity of convective storms in Finland. Meteorological Applications 21, 656–674. https://doi.org/10.1002/met.1389

Ryzhkov, A.V., Schuur, T.J., Burgess, D.W., Heinselman, P.L., Giangrande, S.E., Zrnic, D.S., 2005. The Joint Polarization Experiment: Polarimetric rainfall measurements and hydrometeor classification. Bulletin of the American Meteorological Society 86, 809–824.

Saltikoff, E., Friedrich, K., Soderholm, J., Lengfeld, K., Nelson, B., Becker, A., Hollmann, R., Urban, B., Heistermann, M., Tassone, C., 2019. An overview of using weather radar for climatological studies: Successes, challenges, and potential. Bulletin of the American Meteorological Society 100, 1739–1752.

Saltikoff, E., Huuskonen, A., Hohti, H., Koistinen, J., Järvinen, H., 2010. Quality assurance in the FMI Doppler Weather Radar Network. Boreal environ. res. 15, 579–594.

Saltikoff, E., Lopez, P., Taskinen, A., Pulkkinen, S., 2015. Comparison of quantitative snowfall estimates from weather radar, rain gauges and a numerical weather prediction model.

Schneebeli, M., Grazioli, J., Berne, A., 2013. Improved estimation of the specific differential phase shift using a compilation of Kalman filter ensembles. IEEE transactions on geoscience and remote sensing 52, 5137–5149.
Serafin, R.J., Wilson, J.W., 2000. Operational Weather Radar in the United States: Progress and Opportunity. Bulletin of the American Meteorological Society 81, 501–518. https://doi.org/10.1175/1520-0477(2000)081<0501:OWRITU>2.3.CO;2
Seroka, G.N., Orville, R.E., Schumacher, C., 2012. Radar Nowcasting of Total Lightning over the Kennedy Space Center. Weather and Forecasting 27, 189–204. https://doi.org/10.1175/WAF-D-11-00035.1
Siting Classification | World Meteorological Organization [WWW Document], n.d. URL https://community.wmo.int/activity-areas/imop/siting-classification (accessed 3.31.22).
Stepek, A., Wijnant, I.L., van der Schrier, G., van den Besselaar, E.J.M., Klein Tank, A.M.G., 2012. Severe wind gust thresholds for Meteoalarm derived from uniform return periods in ECA&D. Natural Hazards and Earth System Sciences 12, 1969–1981. https://doi.org/10.5194/nhess-12-1969-2012
Stolzenburg, M., 1994. Observations of high ground flash densities of positive lightning in summertime thunderstorms. Monthly weather review 122, 1740–1750.
Stull, R. (Roland), 2016. Practical Meteorology: an algebra based survey of atmospheric science, https://www.eoas.ubc.ca/books/Practical_Meteorology/. BC Campus.
Tabari, H., 2020. Climate change impact on flood and extreme precipitation increases with water availability. Scientific reports 10, 1–10.
Tabary, P., 2007. The new French operational radar rainfall product. Part I: Methodology. Weather and forecasting 22, 393–408.
Tamm, O., Saaremäe, E., Rahkema, K., Jaagus, J., Tamm, T., 2023. The intensification of short-duration rainfall extremes due to climate change–Need for a frequent update of intensity–duration–frequency curves. Climate Services 30, 100349.
Tammets, T., Jaagus, J., 2013. Climatology of precipitation extremes in Estonia using the method of moving precipitation totals. Theor Appl Climatol 111, 623–639. https://doi.org/10.1007/s00704-012-0691-1
Tammets, T., Jakovleva, O., 2001. Intensity of Estonian rains. Year-book of the Estonian Geographical Society 33, 77–88.
Tammets, T., Paljak, T., Merilain, M., Meitern, H., Mätlik, O., Klaus, L., Kovalneko, O., Vahter, I., Pedassaar, E., Tillmann, E., 2012. Eesti ilma riskid. Eesti Meteroloogia ja Hüdroloogia Instituut: Eesti Entsüklopeediakirjastus.
Thorndahl, S., Nielsen, J.E., Rasmussen, M.R., 2014. Bias adjustment and advection interpolation of long-term high resolution radar rainfall series. Journal of Hydrology 508, 214–226. https://doi.org/10.1016/j.jhydrol.2013.10.056
Tiranti, D., Cremonini, R., Sanmartino, D., 2021. Wildfires Effect on Debris Flow Occurrence in Italian Western Alps: Preliminary Considerations to Refine Debris Flow Early Warnings System Criteria. Geosciences 11, 422. https://doi.org/10.3390/geosciences11100422
Touma, D., Michalak, A.M., Swain, D.L., Diffenbaugh, N.S., 2018. Characterizing the Spatial Scales of Extreme Daily Precipitation in the United States. Journal of Climate 31, 8023–8037. https://doi.org/10.1175/JCLI-D-18-0019.1
Tuomi, T.J., Mäkelä, A., 2007. Salamahavainnot 2007-Lightning observations in Finland, 2007.
Ukkola, A.M., Kauwe, M.G.D., Roderick, M.L., Abramowitz, G., Pitman, A.J., 2020. Robust Future Changes in Meteorological Drought in CMIP6 Projections Despite

Uncertainty in Precipitation. Geophysical Research Letters 47, e2020GL087820. https://doi.org/10.1029/2020GL087820
Vajda, A., Tuomenvirta, H., Juga, I., Nurmi, P., Jokinen, P., Rauhala, J., 2014. Severe weather affecting European transport systems: the identification, classification and frequencies of events. Natural Hazards: Journal of the International Society for the Prevention and Mitigation of Natural Hazards 72, 169–188.
Vulpiani, G., Montopoli, M., Passeri, L.D., Gioia, A.G., Giordano, P., Marzano, F.S., 2012. On the use of dual-polarized C-band radar for operational rainfall retrieval in mountainous areas. Journal of Applied Meteorology and Climatology 51, 405–425.
Waldvogel, A., Federer, B., Grimm, P., 1979. Criteria for the detection of hail cells. Journal of Applied Meteorology and Climatology 18, 1521–1525.
Wilks, D.S., 2011. Statistical methods in the atmospheric sciences. Academic press.
Wilson, J.W., Schreiber, W.E., 1986. Initiation of Convective Storms at Radar-Observed Boundary-Layer Convergence Lines. Monthly Weather Review 114, 2516–2536. https://doi.org/10.1175/1520-0493(1986)114<2516:IOCSAR>2.0.CO;2
Workman, E.J., Reynolds, S.E., 1949. Electrical activity as related to thunderstorm cell growth. Bulletin of the American Meteorological Society 30, 142–144.
Yan, H., Sun, N., Chen, X., Wigmosta, M.S., 2020. Next-generation intensity-duration-frequency curves for climate-resilient infrastructure design: Advances and opportunities. Frontiers in Water 2, 545051.
Yano, J.-I., Ziemiański, M.Z., Cullen, M., Termonia, P., Onvlee, J., Bengtsson, L., Carrassi, A., Davy, R., Deluca, A., Gray, S.L., Homar, V., Köhler, M., Krichak, S., Michaelides, S., Phillips, V.T.J., Soares, P.M.M., Wyszogrodzki, A.A., 2018. Scientific Challenges of Convective-Scale Numerical Weather Prediction. Bulletin of the American Meteorological Society 99, 699–710. https://doi.org/10.1175/BAMS-D-17-0125.1

SUMMARY IN ESTONIAN

Kaksikpolarimeetrilise ilmaradari pikaajaline andmestik aitab tuvastada ja lühiennustada konvektiivseid torme, tugevaid sademeid, äikest ja rahet

Kliimasoojenemisega seoses muutuvad sagedasemaks ja tugevamaks ka sademetega seotud ohtlikud ilmastikunähtused, mis kujutavad endast üha kasvavat riski kogu maailmas. Radariandmete eeliseid on juba tõestatud eelkõige väikesemõõtmeliste ja kiirelt arenevate nähtuste puhul, mis jääksid märkamatuks traditsiooniliste vaatlusjaamade poolt. Sellised nähtused on näiteks konvektiivsed tormid, millega omakorda kaasnevad tugevad vihmavalingud, äike ja rahe. Seni on nende uurimiseks kasutatud valdavalt horisontaalse polarisatsiooniga radareid ja lühikesi aegridu. Kaksikpolarimeetrilistel radaritel on eelmise põlvkonna ees mitmeid potentsiaalseid eeliseid, nagu näiteks täpsem sajukoguste ja sademeliikide hindamine. Selleks, et neid eeliseid kasutada, on vaja piisavalt pikki andmeridasid algoritmide valideerimiseks. Kuigi Eestis on ühed Euroopa pikimad sellist tüüpi operatiivsete radarite aegread, puudusid vastavasisulised uuringud. Käesoleva töö eesmärkideks on

1. Defineerida lähtuvalt radariandmetest Eesti tingimustes konvektiivne torm ja leida konvektiivsete tormide klimatoloogia;
2. Täiustada radaril põhinevat kvantitatiivset sajuhinnangut kasutades kaksikpolarimeetrilisi andmeid;
3. Täiendada Eesti ekstreemsademete klimatoloogiat ja arvutada lühiajaliste tugevate sadude korduvusperioodid;
4. Leida parimad radariandmetel põhinevad äikest ja rahet detekteerivad parameetrid.

Kasutades konvektiivsete sajualade eristamiseks Sürgavere radari peegelduvust ja konvektiivsete keskkonnatingimuste tuvastamiseks atmosfääri järelanalüüsi mudelandmete konvektiivset kättesaadavat energiat CAPE (*Convective Available Potential Energy*), defineeriti konvektiivne torm kui ala, kus peegelduvus ≥ 51 dBZ ja CAPE ≥80 J/kg. Aastate 2010–2019 (v.a. 2017) andmete põhjal leiti, et kõige suurem konvektiivse tormi esinemise tõenäosus on, kui õhuvool on kagust (62%) või lõunast (60%). Uuritud perioodil vahemikus mai algusest kuni septembri lõpuni määrati konvektiivne torm kusagil Eesti territooriumil peaaegu pooltel päevadel (45%), pilv-maa välkudega päevad olid veel sagedasemad (54%). Enim esines torme Mandri-Eesti lääne- ja edelaosas (kuni 8 tormipäeva aastas 100 km^2 võrguruudu kohta) ja vähim Lääne-Eesti saarestikus (2 tormipäeva 100 km^2 kohta). Aladel, mis jäid radari asukohast kaugemale kui 100 km, detekteeriti üldiselt vähem torme ka radarile iseloomuliku kauguse suurenedes lisanduva madalama täpsuse tõttu.

Radariandmetel põhinevad kvantitatiivsed sajuhinnangud arvutati kolme erinevat meetodit kasutades viie aasta suveperioodi (mai algusest septembri lõpuni) andmete põhjal. Sademete akumulatsioonid arvutati 1 tunni, ööpäeva ja kuu sammuga. Kõikide perioodide keskmisena oli jaamades mõõdetud sajukogustega võrreldes kõige täpsem horisontaalset peegelduvust ja spetsiifilist diferentsiaalset faasi kombineeriv meetod (Pearsoni korrelatsioonikoefitsient 0,800, normaliseeritud keskmine kõrvalekalle 0,250). Horisontaalsel peegelduvusel põhinev meetod alahindas sajukoguseid (normaliseeritud keskmine kõrvalekalle –0,159), eriti tugevamate sadude korral ja ainult spetsiifilist diferentsiaalset faasi kasutav meetod jällegi ülehindas tugevalt (1,731), eriti just väiksemate sajukoguste puhul. Samu meetodeid rakendati ka ekstreemsademete klimatoloogia arvutustes, kus esmalt leiti 1 tunni sademete akumulatsiooni aastamaksimumid ja nende põhjal teatud intensiivsusega sademete esinemise korduvusperioodid. Kuna see seadis kõrgemad nõudmised andmete kvaliteedile, oli vaja spetsiifilise diferentsiaalse faasi arvutusmeetodit parendada. Tulemused kinnitasid, et ka lühiajaliste ekstreemsademete puhul on kõige täpsem kombineeritud meetod (horisontaalne peegelduvus ja spetsiifiline diferentsiaalne faas) ja vaid 5 aasta radariandmete põhjal on võimalik leida korduvusperioode kuni 100 aasta kohta eeldusel, et sademete klimatoloogia on kogu piirkonnas samasugune. Saadud tulemusi saab kasutada hüdroloogilistes rakendustes ja need aitavad panna Eestis kasutatavad tugevate sademete hoiatuskriteeriumid esinemissageduse perspektiivi.

Selleks, et leida äikest ja rahet detekteerivad parimad parameetrid, kasutati 4 aasta andmeid vahemikust 2011–2014 ja määrati esmalt konvektiivsed sajualad, kasutades 35 dBZ radari peegelduvuse piiri. Seatud piirmäär valiti piisavalt madal, et hõlmata ka nõrgemaid torme. Leitud aladest 33,9% sisaldas pilv-maa välgulööke ja 25,9% rahet. Neid väärtuseid võib pidada ka nende nähtuste esinemise tõenäosuseks, kui peegelduvuse väärtus ületab 35 dBZ. Kokku võrreldi 16 erinevat radariandmetel põhinevat parameetrit ja leiti, et parim pilv-maa välgu indikaator oli 20 dBZ peegelduvuse kõrgus ja rahe detekteerimiseks oli parim sajuala maksimaalne peegelduvus.

Doktoritöö tulemused näitavad, et pikaajalist operatiivse kaksikpolarimeetrilise radari andmestikku kasutades on võimalik tõsta suviste ohtlike ilmastikunähtuste määramise täpsust ja hinnata hüdroloogilisi riske. Töö tulemustel on suur praktiline väärtus ja neid saab võtta operatiivsesse kasutusse konvektiivsete tormide detekteerimiseks ja lühiennustuste koostamiseks. Samuti on käesolev töö oluliseks aluseks radarmeteoroloogia-alastele edasistele töödele Eestis.

ACKNOWLEDGEMENTS

First and foremost I would like to thank my supervisors Dr Piia Post and Dr Dmitri Moisseev for their support throughout my PhD studies. I am very grateful for their time and effort they put into scientific discussions and reviewing my work. Their patience with me and keen interest in my progress is highly appreciated.

I wish to thank everyone in the Atmospheric Physics Lab in the University of Tartu for providing a supporting environment to writing the thesis. Special gratitude goes to Jorma Rahu, who has been an irreplaceable companion in developing the weather radar field in Estonia. I thank all the coauthors of the research papers included in this thesis for their time and effort: Roberto Cremonini, Tuule Müürsepp, Pekka Rossi and Tarmo Tanilsoo. I also wish to thank Jussi Haapalainen from the Finnish Meteorological Institute for helping with the NORDLIS lightning data. I am grateful to my employer the Estonian Environment Agency for my interesting work position, providing the radars and the data to work with and all the colleagues there who have given helpful insights into the field.

I am deeply thankful to my parents for their patience and support and giving me the thirst for knowledge and encouraging my interest in weather from an early age. I thank my sister and brothers, who have always been my best friends. Lastly, I cannot thank enough my wife Liina who has helped me come through all the ups and downs during these studies and provided endless support.

This work was supported by research grant No. 9140 from the Estonian Science Foundation; institutional research funding IUT20-11 from Estonian Research Council; personal research grants No. PSG202 and PRG1726 from Estonian Research Council and the European Regional Development Fund within the National Programme for Addressing Socio-Economic Challenges through R&D (grant No. RITA1/02-52-07).

PUBLICATIONS

CURRICULUM VITAE

Name: Tanel Voormansik
Date of birth: 15.11.1989
Citizenship: Estonian
Gender: Male
E-mail: tanel.voormansik@ut.ee

Education

2014–2023 University of Tartu, PhD in Environmental Technology
2012–2014 University of Tartu, MSc in Environmental Technology
2009–2012 University of Tartu, BSc in Environmental Technology

Languages

Estonian (native speaker), English (fluent in speaking and writing), Russian (basic), Finnish (basic)

Professional employment

2012–… Estonian Environment Agency, Senior specialist, radar meteorology
2014–… University of Tartu, Engineer

Research interests

Natural sciences and engineering, atmosphere physics, climatology, radar meteorology, remote sensing

Publications

Cremonini, R., **Voormansik, T**., Post, P. and Moisseev, D., 2023. Estimation of extreme precipitation events in Estonia and Italy using dual-polarization weather radar quantitative precipitation estimations. Atmospheric Measurement Techniques 16(11), 2943–2956.

Voormansik, T., Müürsepp, T., Post, P. 2022. Konvektiivsete tormide klimatoloogia Eestis lähtuvalt radariandmetest ja keskkonnatingimustest. Kaugseire Eestis 2022, 99–108.

Voormansik, T., Müürsepp, T., Post, P., 2021. Climatology of convective storms in Estonia from radar data and severe convective environments. Remote Sensing 13(11), 2178.

Voormansik, T., Cremonini, R., Post, P., Moisseev, D., 2021. Evaluation of the dual-polarisation weather radar quantitative precipitation estimation using long-term datasets. Hydrology and Earth System Sciences 25(3), 1245–1258.

Rahu, J., **Voormansik, T.**, Post, P., 2018. Enhancement of radar rainfall estimates for Estonian territory through optical flow temporal interpolation. ERAD 2018 Book of Abstracts: 10th European Conference on Radar in Meteorology and Hydrology (ERAD 2018): 1–6 July 2018, Ede-Wageningen, The Netherlands.

Voormansik, T., Rossi, P.J., Moisseev, D., Tanilsoo, T., Post, P., 2017. Thunderstorm hail and lightning detection parameters based on dual-polarisation Doppler weather radar data. Meteorological Applications 24(3), 521–530.

Paljak, T., Toll, V., **Voormansik, T.**, 2016. Large hail in Estonia on 12th August 2015. European Forecaster, 21, 26–30.

Männik, A., Toll, V., **Voormansik, T.**, 2014. Sirgäikesetorm 8. augustil 2010 satelliitidelt ja radaritelt nähtuna. Kaugseire Eestis 2014, 166–174.

ELULOOKIRJELDUS

Nimi: Tanel Voormansik
Sünniaeg: 15.11.1989
Kodakondsus: Eestlane
Sugu: Mees
E-mail: tanel.voormansik@ut.ee

Haridus

2014–2023	Tartu Ülikool, keskkonnatehnoloogia õppekava, PhD
2012–2014	Tartu Ülikool, keskkonnatehnoloogia õppekava, MSc
2009–2012	Tartu Ülikool, keskkonnatehnoloogia õppekava, BSc

Keelteoskus

Eesti (emakeel), inglise (suurepärane kõnes ja kirjas), vene (baastase), soome (baastase)

Töökogemus

2012–…	Keskkonnaagentuur, peaspetsialist, radarmeteoroloogia
2014–…	Tartu Ülikool, insener

Teadustöö põhisuunad

Loodusteadused ja tehnika, atmosfäärifüüsika, klimatoloogia, radarmeteoroloogia, kaugseire

Publikatsioonid

Cremonini, R., **Voormansik, T**., Post, P. and Moisseev, D., 2023. Estimation of extreme precipitation events in Estonia and Italy using dual-polarization weather radar quantitative precipitation estimations. Atmospheric Measurement Techniques 16(11), 2943–2956.

Voormansik, T., Müürsepp, T., Post, P. 2022. Konvektiivsete tormide klimatoloogia Eestis lähtuvalt radariandmetest ja keskkonnatingimustest. Kaugseire Eestis 2022, 99–108.

Voormansik, T., Müürsepp, T., Post, P., 2021. Climatology of convective storms in Estonia from radar data and severe convective environments. Remote Sensing 13(11), 2178.

Voormansik, T., Cremonini, R., Post, P., Moisseev, D., 2021. Evaluation of the dual-polarisation weather radar quantitative precipitation estimation using long-term datasets. Hydrology and Earth System Sciences 25(3), 1245–1258.

Rahu, J., **Voormansik, T.**, Post, P., 2018. Enhancement of radar rainfall estimates for Estonian territory through optical flow temporal interpolation. ERAD 2018 Book of Abstracts: 10th European Conference on Radar in Meteorology and Hydrology (ERAD 2018): 1–6 July 2018, Ede-Wageningen, The Netherlands.

Voormansik, T., Rossi, P.J., Moisseev, D., Tanilsoo, T., Post, P., 2017. Thunderstorm hail and lightning detection parameters based on dual-polarisation Doppler weather radar data. Meteorological Applications 24(3), 521–530.

Paljak, T., Toll, V., **Voormansik, T.**, 2016. Large hail in Estonia on 12th August 2015. European Forecaster, 21, 26–30.

Männik, A., Toll, V., **Voormansik, T.**, 2014. Sirgäikesetorm 8. augustil 2010 satelliitidelt ja radaritelt nähtuna. Kaugseire Eestis 2014. (166–174).

DISSERTATIONES GEOPHYSICALES UNIVERSITATIS TARTUENSIS

1. **Andres Kuusk.** The hot-spot effect in plant canopy reflectance. Tartu, 1991.
2. **Tiit Nilson.** Radiative transfer in non-homogeneous plant canopies. Tartu, 1991.
3. **Helgi Arst.** Atmosfääri ja mere kiirguskarakteristikud looduskeskkonna seisundi informaatoritena (vene keeles). Tartu, 1991.
4. **Juha Sarkkula.** Measuring and modelling water currents and quality as a part of decision making process for water pollution control. Tartu, 1992.
5. **Piia Post.** On the two radiatively effective cloud parameters. Tartu, 1993.
6. **Aadu Mirme.** Electric aerosol spectrometry. Tartu, 1994.
7. **Aare Luts.** Mathematical simulation of the evolutions of air ions. Tartu, 1995.
8. **Tiit Kutser.** Estimation of water quality in turbid inland and coastal waters by passive optical remote sensing. Tartu, 1997.
9. **Ülle Kikas.** Atmospheric aerosol in the Baltic region. Tartu, 1998.
10. **Tarmo Kõuts.** Processes of deep water renewal in the Baltic sea. Tartu, 1999.
11. **Anu Reinart.** Underwater light field characteristics in different types of Estonian and Finnish lakes. Tartu, 2000.
12. **Marko Kaasik.** Parameterisation of atmospheric boundary layer in the numerical model of air pollution transport. Tartu, 2000.
13. **Janek Laanearu.** Topographically constrained deep-water flows in channels. Tartu, 2001.
14. **Urmas Raudsepp.** Wind-driven circulation in the gulf of Riga. Tartu, 2001.
15. **Urmas Hõrrak.** Air ion mobility spectrum at a rural area. Tartu, 2001.
16. **Marko Vana.** Formation and evolution of atmospheric aerosol size spectrum by the occurrence of nucleation burst events in the atmospheric boundary layer; transport of the climatically active particulate air pollution. Tartu, 2002.
17. **Veljo Kimmel.** Analysis of methods of air quality assessment. Applications in Estonia. Tartu, 2002.
18. **Oleg Okulov.** Variability of atmospheric transparency and precipitable water in Estonia. Tartu, 2003.
19. **Aarne Männik.** Implementation and validation of the nonhydrostatic adiabatic core of the numerical weather prediction model hirlam. Tartu, 2003.
20. **Matti Mõttus.** Shortwave solar radiation field inside willow canopy. Tartu, 2004.
21. **Kalev Rannat.** Long weakly nonlinear waves in geophysical applications. Tartu, 2007.
22. **Rigel Kivi**. Observations of ozone, polar stratospheric cloud and water vapour profiles in the arctic. Tartu, 2007.

23. **Erko Jakobson.** Spatial and temporal variability of atmospheric column humidity. Tartu, 2009, 125 p.
24. **Sander Mirme.** Development of nanometer aerosol measurement technology. Tartu, 2011, 118 p.
25. **Hannes Keernik.** Estimating methods and variability of atmospheric humidity over the Baltic Region and the Arctic. Tartu, 2015, 105 p.
26. **Martin Kannel.** Development of Broadband Aerosol Optical Depth Models. Tartu, 2016, 168 p.
27. **Krista Alikas**. From research to applications: monitoring optically complex waters with MERIS/ENVISAT data. Tartu, 2016, 172 p.
28. **Velle Toll.** Direct radiative impacts of atmospheric aerosols on meteorological conditions over Europe. Tartu, 2016, 148 p.
29. **Margit Aun.** Dependence of UV radiation on climate factors. Reconstruction of UV doses in Estonia for past years. Tartu, 2017, 124 p.
30. **Siiri Suursoo.** Natural Radioactivity in Cambrian-Vendian Groundwater – Analytical Procedures, Monitoring of Drinking Water Treatment Technology, and Associated Changes in Groundwater Quality. Tartu, 2019, 146 p.
    Heido Trofimov. Polluted clouds at air pollution hot spots help to better understand anthropogenic impacts on Earth's climate. Tartu, 2022, 144 p. Published in *Dissertationes Physicae Universitatis Tartuensis*, 128 p.